Doctoral theses at NTNU, 2020:406

Terje Solbakk

Different aspects of detecting karst with geophysical methods – Tales from the underworld

Doctoral thesis

NTNU
Norwegian University of Science and Technology
Thesis for the Degree of
Philosophiae Doctor
Faculty of Engineering
Department of Geoscience and Petroleum

NTNU
Norwegian University of
Science and Technology

Terje Solbakk

Different aspects of detecting karst with geophysical methods – Tales from the underworld

Thesis for the Degree of Philosophiae Doctor

Trondheim, December 2020

Norwegian University of Science and Technology
Faculty of Engineering
Department of Geoscience and Petroleum

NTNU
Norwegian University of Science and Technology

NTNU
Norwegian University of Science and Technology

Thesis for the Degree of Philosophiae Doctor

Faculty of Engineering
Department of Geoscience and Petroleum

ISBN 978-82-471-9466-9 (printed ver.)
ISBN 978-82-471-9967-1 (electronic ver.)
ISSN 1503-8181 (printed ver.)
ISSN 2703-8084 (online ver.)

Doctoral theses at NTNU, 2020:406

Printed by NTNU Grafisk senter

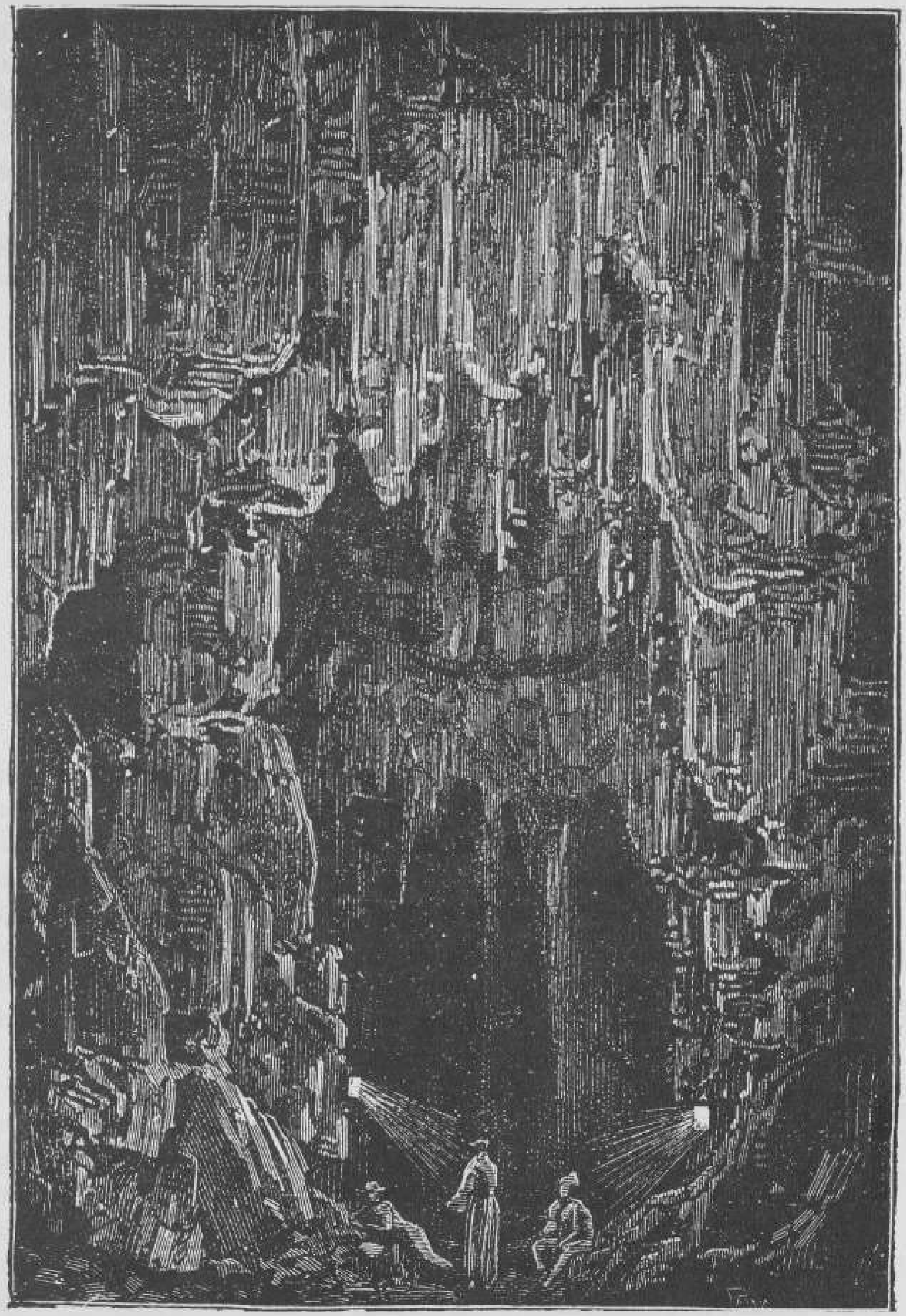

Jeg? Under jorden? Slik at vi kan bli sittende fast i en av disse fuktigkalde labyrintene av noen grotter og aldri mer får se dagens lys? Aldri!

"Me? Under the earth? So that we may be stuck in one of these moist-cold labyrinths of some caves and nevermore see the light of day? Never!"

Jules Verne, 1864: Voyage au centre de la Terre*, Den norske bokklubben (Norwegian edition, 1967 (5th edition, 1976) with image reproduced from the original French edition (artist not given).*

Errata, corrected as of 25th of November 2020:

- Page 11: first sentence deleted in paragraph ("In this section, a coarse overview of the age of deposition of likely candidates for karstification in Norway is given").
- Page 102: Last sentence on page rewritten to clarify meaning.
- Page 129, line 17: reference corrected to Table 3 instead of Table 2.
- Page 130, line 14: well number corrected to 6608/8-1 from 66608/8-1.
- Page 136, line 18: "precipitation" changed to "dissolution".

Acknowledgements

This work has been carried out at the Department of Geoscience and Petroleum at the Norwegian University of Technology and Science (NTNU) in Trondheim. I am very grateful for the assistance, guidance, trust, confidence and constructive comments from my main supervisor Philip Ringrose and my co-supervisors Christine Fichler and Tore Amund Svånå. I am grateful for the support and cooperation with Walter Wheeler (Norce, Bergen) and Stein-Erik Lauritzen (University of Bergen) in the making of article no. 1. I also appreciate the support and input from fellow PhD candidates and postdocs at NTNU, especially Carlos Aizprua Luna, Dicky Harishidayat and Kamaldeen Omosanya. For assisting, guiding and explaining different parts of the NTNU PhD system to me, I truly appreciate Sylvi Vefsnmo and the administration staff at IGP and Runa Nilssen at the faculty; and I must not forget to thank the head of department Egil Tjåland for kicking me into the geoblog business.

Through the ARCEx Research Centre that financed my PhD, I met academic colleagues from all over Norway; especially, the Early Career Forum gatherings and Annual ARCEx meetings were of great inspiration to me. There I got constructive feedback on my work, met amazing people and most importantly: I will never forget the two persons who were extremely helpful at a time when it was most needed: Ellen Hætta and Alfred Johansen: Thank you so much!

I would also like to thank Ida Margrethe Meling, Odd Bakke Kristiansen, and Nils Rune Sandstå at the NPD for granting permission and for approving geological sampling, access to the NPD Core store, and for assistance in return of samples. I also thank former colleagues at the NPD for believing in me when I quit my job there and moved to Trondheim.

Odleiv Olesen (NGU) is thanked for the invitation to be a part of the program committee and to hold a presentation at the seminar “Leiromvandling på Norsk sokkel, hvor og hvorfor”, 23rd of May 2016. Marco Brönner (NGU) is thanked for discussion and access to gravity and magnetic data from the Barents Sea. Morten Smelror (NGU) is thanked for positivity, fieldwork, invitation to reports and the invitation to cowrite a scientific note, on a for me surprising discovery of trace fossils in my local area, and not to forget the possibility to talk at the Nordic Geological Winter meeting in January 2020 on another, very surprising discovery of Mesozoic palynomorphs in a karst landscape, together with Harald Brunstad from Lundin and Ingard Throndsen from Applied Petroleum Technology AS. Trøndelag is full of geological wonders yet to be discovered!

Also, I will not forget the karst enthusiasm and support of Harald Brunstad and to his many colleagues that I met at Lundin Petroleum Norway AS: for the invitation to guide you on field excursions in 2016 and 2018, for the arrangement of analyses of the samples from the field trip, for lending me 3D data and for the invitation to come and speak to you in Oslo.

During the PhD, Arne Grønlie from Aker BP has provided plenty of karst enthusiasm, scientific discussions and evening hikes to the Forbordsfjell mountain and elsewhere in all kinds of weather. Together with his colleagues we also had a great time at the 2018-field excursion in the mountains near Mo i Rana.

Halfdan Carstens and Ronny Setså at Geopublishing are thanked for constructive feedback and support of my texts that were published at Geoforskning.no. Let’s spread the gospel of the true meaning of the term “Nord-Europa”.

Karsten Eig and Bjørn Egil Johansen are thanked for their often constructive, sometimes sarcastic and all the time honest opinions on bits and pieces of my manuscript texts suddenly appearing to them in Facebook Messenger chat boxes. What are friends for, if not to torment?

And to family and friends for support and interest, and not to forget the laconic question from my dad: “Ja, ka fan ska du bi når du bi ferdi?”…

My dearest wife Ingvild for love, support and for being a safe harbor in rough weather.

To our daughter Tora, for everything so far and for the years to come.

Terje Solbakk

Stjørdal, September 2020

Abstract

The work in this thesis integrate conventional seismic interpretation, gravity survey data, field data from analogues and state-of-the-art numerical modeling in order to broaden and increase the understanding of the distribution of porosity and permeability derived from chemical dissolution of rocks (karst). Karst porosity from small scales to the large are addressed onshore Norway (Paper 1), the intermediate scale in the offshore setting of the Loppa High, Barents Sea (Paper 2) and the large scale encompassed the entity of both land and offshore areas of Norway (Paper 3). All papers present new workflows combining geophysical methods and geology for karst mapping and prediction. Furthermore, challenges related to distinguishing pseudokarst from karst were addressed in the two offshore papers (Paper 2 and 3), as well as the geophysical imaging problems related to isomorphs (Paper 2).

The first case study area (Paper 1) includes onshore Norway's largest cave room, within the Svarthammarhola cave system (SHC), located in a Caledonian nappe setting in Nordland. This is the first time microgravimetric data is used for mapping of known and detection of hitherto unknown karst cave passages in Norway, and a workflow is presented for interpretation of assumed karst. Cave passages and karst features of the Svarthammarhola cave, form negative density contrasts expressed in gravity field anomalies. Here, microgravimetric methods are shown to be applicable in challenging geological settings with heterogeneous lithologies. This setting is a good onshore analogue which is highly applicable for offshore settings. Challenges due to heterogeneous infill of large cavities and variations in carbonate facies are also addressed. The workflow covers not only the detection of large cave rooms, but also deals with minor karst features (epikarst) in carbonate rocks. A 3D density model was built utilizing 3D forward modelling aiming on matching model with surface gravity measurements. The most important result relates to distinct gravity lows detected in the survey, which are interpreted as formerly unknown and inaccessible cave rooms, some of them of an exceptionally large size. These correspond with known collapse and sediment infill features both at the surface and inside the Svarthammarhola cave. This expands the known cave in an eastward and northward direction. One thought-provoking insight is the cave's position at the top of the hinge of a large antiform combined with uncommonly high densities in parts of the host-rocks. These observations, together with the cave's outstanding size, lead to different interpretations regarding the speleogenesis of the Svarthammarhola cave. These interpretations include both meteoric and hypogene karst likely related to hypogenic fluids from deep-seated hotter aqueous flow systems, generally related to tectonic or volcanic systems.

Paper 2 deals with different aspects of detecting submerged karst porosity in carbonate rocks using seismic imaging. Several challenges are addressed related to the identification of karst elements and karst landforms. This includes the size distribution of the cavities, the resolution capability of seismic data, the geological history leading to different types of karst infill, and the differentiation from other features which give similar seismic expressions (isomorphs). An important observation here is that identifying karst-like morphology on seismic reflection data alone is not sufficient to prove karstification. The seismic expression needs to be integrated with geological interpretation, and alternative isomorph interpretations need to be assessed. In this paper, the nature of karst features with their seismic expression is reviewed, and potential isomorphs are assembled. Two case studies from the Loppa High of the Barents Sea are presented, where two regions were identified: one with clear karst expressions on seismic data supported by secondary arguments, and one with more equivocal interpretations where alternative models may be valid. The implications of these alternative karst models for hydrocarbon exploration studies are shown to be significant, especially if expected karst-related high porosity zones in fact are absent.

Paper 3 unravels karst potential by providing a summary of where to find karst features buried on the NCS and where there is karst potential. Karst (paleokarst) features are occasionally reported in exploration wells throughout the NCS. Still, the contribution of karst porosity to the overall porosity of potential reservoir rocks is highly variable. Meteoric fluids stand out as the primary agents for karstification in this setting, but also hypogene fluids may be expelled upwards during phases of tectonic activity and presumably along deep-seated fault zones. The most promising karst play on the NCS are likely to be found in Late-Paleozoic limestones. Karst in chalk may have a potential upside in the eastern North Sea. Paleokarst may also be found in Caledonian basement terrane, as proven from one well in the Norwegian Sea. The paper also briefly discusses other tertiary porosity elements, such as silicate karst and other pseudokarst features, which might represent a potential upside in reservoir porosity.

Contents

Introduction

Objectives and scope

Generally, weathering of rocks is manifested in many ways - from physical weathering by e.g. rivers, waves, and gravity, to chemical weathering. Chemical weathering, more specifically chemical dissolution of limestone, is the focus of this thesis as captured by the term “karst”.

Karst porosity is common in hydrocarbon reservoirs in carbonates around the world, see e.g., Bauer & Tóth (2017), Bourdon *et al.* (2004), Clark (1986), Craig (1990), Kerans (1988), Lomando *et al.* (1993), Lapointe *et al.* (2002), Shi *et al.* (2014), Tian *et al.* (2016), and Yu *et al.* (2018).

The understanding of karst porosity, with caves as its most prominent expression, has during the last decade attracted focus on the Norwegian Continental Shelf (NCS) (www.factpages.npd.no).

Recent discoveries have proven hydrocarbons in carbonate reservoirs: With the discovery wells 7120/3-1 ‘Gohta’ and 7220/11-1 ‘Alta’ in the southwestern Barents Sea, moveable oil and gas have been proven in reservoir rocks with good tertiary porosity from karst dissolution (press releases at npd.no). Karstified reservoirs are important for further exploration on the NCS, even though commercialization of the mentioned discoveries is not decided upon at this stage. Karstified reservoirs on the NCS have up to now been under-explored. The reasons for this relate to:

A. The challenge of recognizing karst weathering on seismic data. In the literature, this identification is mostly done based on morphological resemblance and a priori knowledge of bedrock at reservoir level – see e.g. Bourdon *et al.* (2004), Fournillon *et al.* (2017); Hunt *et al.* (2003), Sayago *et al.* (2012), Sayago *et al.* (2014); Sayago *et al.* (2018); Tian *et al.* (2016), Vahrenkamp *et al.* (2004), Xu *et al.* (2016); Yu *et al.* (2018) and Zeng *et al.* (2011). Some recent seismic interpretations of offshore karst on the Norwegian Continental Shelf (NCS) (caves, dolines, and epikarst) by Ahlborn *et al.* (2014), Hunt *et al.* (2003), Hunt *et al.* (2010), Rafaelsen *et al.* (2008), Sayago *et al.* (2012), and Sorento *et al.* (2018), are also reported. It is conspicuous that in these papers, alternative explanations for karst-like features are rarely considered when interpreting morphological features on seismic reflection data in carbonate formations assigned to karst. This approach may turn out to be a pitfall as it often ignores other possible explanations for the same buried landforms. Such alternative explanations are here referred to as isomorphs. According to Halliday (2007), a variety of non-dissolutional processes forms terrains analogous to certain types of karst; these are termed pseudokarst.

In this thesis a major task has been to distinguish karst from pseudokarst, and in geophysical data to distinguish karst from non-karst expressions (isomorphs).

B. Limited information from well samples. Drilled cores taken when drilling a subsea reservoir can be used to predict lithology and the overall reservoir quality, including permeability and porosity, which is a well-established practice. However, such interpolation from well samples is somewhat limited in applicability on a larger scale around the well and will, therefore, lead to an incomplete understanding of the karstified reservoir. This will be especially relevant for karst reservoirs where one expects significant lateral heterogeneity with variations from very high to low porosity and permeability, that may affect both exploration and production forecasts.

Overall, the scope for this thesis is to broaden and increase the understanding of the distribution of porosity and permeability derived from chemical dissolution of rocks (karst), in settings where geophysical methods are needed to entangle e.g. hydrocarbon reservoir properties or groundwater distribution. The workflows presented may also be applicable to reservoirs with e.g. deep weathering (e.g. Migon & Lidmar-Bergström, 2002). This is done by integrating conventional seismic interpretation, gravity survey data, field data from analogues and state-of-the-art numerical modeling. Fig. 1 shows a compilation of geological and geophysical methods for karst detection, explaining the relevance of the papers presented in this thesis.

Karst detection

		Shallow	Deep
Common geophysical methods	Onshore	• Microgravimetry **(Paper 1)** • Electric resistivity methods (ERT) • Near-surface seismic methods	• Reflection seismic method **(Paper 2 and 3)**
	Offshore	• Gravimetry • Seismic reflection data	• Reflection seismic method **(Paper 2 and 3)**
Geological methods	On- and offshore	• Surface exploration and field analogues **(Paper 1, 2 and 3)**	• Assessment of buried karstifiable rocks and fluid systems **(Paper 2 and 3)**

Figure 1 Summary over suitable methods for karst detection, referenced to work conducted in this thesis numbered by accompanied paper.

The work also aims to contribute to a better understanding of karstified carbonate reservoirs in general.

This is addressed in the following three papers and discussed in the end:

Introduction to Paper 1: Microgravimetry as a method for detection of karst

Several papers demonstrate the use of gravity measurements as an aid to find natural and man-made cavities; either as a standalone method, or combined with other geophysical methods, or by invasive techniques such as drilling or entering the cave. Chico (1964) was the first to go into detail on detection of caves by gravimetry and referred to earlier work pointing to such possibilities. Later, Butler (1984), Barrows and Fett (1985), Styles *et al.* (2005), Ardestani (2008), Martinez-Moreno *et al.* (2014), Braitenberg *et al.* (2015) and Kaufmann, Nielbock and Romanov (2015) showed examples of successfully detecting karst caves, some supported also by other geophysical methods like resistivity imaging and self-potential surveying (Kaufmann, Nielbock and Romanov, 2015) or by drilling (Barrows and Fett, 1985; Ardestani 2008). However, at times, inconclusive results have been reported due to the inherent ambiguity in gravimetric exploration, for example Kaufmann and Romanov (2009) described a case where the gravimetry data could not distinguish between a buried doline and a cave. Epikarst has been considered in earlier work applying gravity data to karst cave exploration, e.g. in connection with seasonal changes in groundwater levels (Jacob *et al.*, 2009).

Microgravimetry as a method for identifying known and previously unknown karst caves in a complex geological setting onshore is tested (Solbakk *et al.*, 2018). (Open) cave passages form negative density contrast expressed in gravity field anomalies. Here, microgravimetry is used to investigate the geometry of hidden cave passages believed to be a continuation of the Svarthammarhola cave system in Nordland, Norway, and the distribution of multiscale karst features.

This is the first time microgravimetric data is gathered and modelled over karstified bedrock in Norway. The age and speleogenesis of the SHC is presently not known, but the present study demonstrate the potential for near-surface mapping and discusses the potential for application in hydrological or petroleum exploration studies, acting as an onshore analogue.

Introduction to Paper 2: Interpretation of karst features on seismic data

Paper 2 concerns interpretation of geophysical signatures of candidate karstic rock formations and suggest possible non-karstic candidates, by comparing deeply buried karst landscape with relict and modern analogs. The aim of this paper is to shine light on karst prediction, to point out that karst-like features in seismic are not necessarily karst and the consequence of the ambivalence of seismic karst-like morphology. This paper addresses the main karst morphological features and point to possible isomorphs. This is exemplified by using two case studies from a submerged structural high, the Loppa High in the Barents Sea. Criteria are established on how to reliably identify elements of the karst landscape. Hopefully, this will further mitigate the understanding of karst in a play model, both as a risk and as a prospective target. With an increasing focus on karstified carbonates as an exploration play over the last years, stimulated by the first potentially commercial discoveries on the western Loppa High in the southwestern Barents Sea, this area was chosen as a case study. Mainly due to its good availability on seismic data and its many available well cores and petrophysical logs. To perform this task, one need to understand the permeability and porosity distribution by using geophysical data in combination with field data. This was be done by the means of interpreting seismic signatures and investigate relationship to chemical weathering using indicators such as paleotopography, paleogeography and eustatic sea level changes. Further, relict, and modern analogs are compared to the submerged karst landscapes of the Loppa High.

Introduction to Paper 3: An overview of karst features on- and offshore Norway

This paper presents an overview of known karst features on the offshore Norwegian Continental Shelf (NCS), together with a summary of large-scale karst features onshore Norway. The compiled database and associated interpretations should form a basis for assessing hitherto unknown karstification in the offshore areas. Although the overall ‘karst play’ on the Norwegian Continental Shelf has been of limited commercial success so far, the comprehensive review complied in Paper 3, should contribute to further assessments of karstified reservoir formations. Karst-prone carbonates are widespread throughout the NCS, and new hydrocarbon plays may well emerge in future. This paper also touches upon chemical dissolution of other rocks and addresses other weathering phenomena, termed pseudokarst (Halliday, 2007).

ARCEx project

This Ph.D. research project is funded by the ARCEx project (Research Centre for Arctic Petroleum Exploration – www.arcex.no) which is funded by the Research Council of Norway (grant number 228107) together with ten academic and nine industry partners, and is part of the ARCEx Work Package 4 (Technology for eco-safe exploration in the Arctic) under Task 4.5 Geophysical imaging of prospects and reservoirs from field analogues on Svalbard and Greenland, with the following overall research goals:

- How seismic signatures of Barents Sea reservoirs can be related to burial and uplift
- How karst systems can be seen in seismic data

These goals are met in this thesis by connecting karst features to their seismic signatures, addressing possible misattributions while interpreting these features. Further, it addresses the karst development under sub-aerial conditions and under later burial conditions where possible influx related to non-surface fluids may add to the overall karst play.

Introduction to karst

Karst describes the processes where landforms evolve due to the chemical dissolution of the host rocks (Ford & Williams, 2007). The definition of karst is discussed by Klimchouk (2015) where it is summarized as: "*Karst (karstic) features (phenomena and forms) – underground and, at certain stages of the evolution, superficial, – are the reflection of the functioning of the karst geohydrodynamic system in the present (active karst features) or in the past (relict karst and paleokarst features).*". Table 1 gives an overview over the most common karst types and definitions.

The process of karstification is associated with rocks susceptible to chemical weathering, most commonly limestone/marble consisting of mainly calcium carbonate ($CaCO_3$), or dolomite ($CaMg(CO_3)_2$) which is formed when Ca^{2+} is substituted by Mg^{2+}. Karst landforms are plentiful, and the most common landforms are caves, dolines and karren (Ford & Williams, 2007).

Caves are likely the best-known landform of karst. Caves, *sensu lato*, are strangely enough hard to define, but *sensu stricto* one can use Ford & Williams' (2007) definition where they state that a karst cave is an opening in a rock enlarged by dissolution where one reaches a diameter sufficient enough for a given hydrodynamic setting to switch from the kinetic state of laminar flow to turbulent flow. This typically happens at openings of 5 – 15 mm diameter/width. The International Speleological Union (www.uis.no) gives a more straightforward practicable definition as an underground opening large enough for human entry, thereby limiting the definition of caves not only to dissolution caves but also by expanding the term to marine abrasion caves, talus deposits *et cetera*. In this thesis caves refer to karst.

Dolines encompass a variety of enclosed depressions ranging from a few meters to km-width and more, they can be considered as diagnostic features of karst terrains. Karren encompasses a vast range of different dissolutional grooves, pits and channel forms, and

Table 1 Table with an explanation of karst types mentioned in the text and papers.

Karst type	*Definition (*Ford & Williams, 2007; **Ford, 1995, ***Halliday, 2007)*
Meteoric	*Meteoric water is the main dissolutional fluid for karstification, either rainwater or groundwater flow or streams**
Hypogene	*Dissolution by fluids from underground sources, either groundwater heated from the deeper earth crust, or acids entering aquifers (Klimchouk, 2018)*
Active	*Karst (caves) under development as part of a still-active karst system**
Fossil	*Karst (caves) formed as part of a still-active karst system, but abandoned by waterways**
Relict	*Karst (caves) with no connection to the present-day hydrological regime**
Paleo	*Karst (caves) with no connection to present-day hydrological regime or landscape***
Pseudo	*Cavities and landforms that are similar to karst landforms but not related to karstification, here used mainly for cavities****

ranges from cm to 10 m in their greatest dimensions for single features. Karren assemblages may cover larger areas, termed karrenfeld.

Karst features are not exclusive to carbonates. In fact, almost all rocks are karstifiable, meaning they can be dissolved by acidic fluids, but this process will act so slow on most rock types, that other erosional processes will out-pace karstification by factors of 10 in time or more (Ford & Williams, 2007). Carbonates and evaporites (gypsum, anhydrite, and salt) can in this matter be identified as easily karstified. Carbonate cement or mixed siliciclastic-limestone may also be susceptible for karstification. Ford & Williams (2007) demonstrate a wide diversity of karst landforms, from millimeter-sized to mega-scale.

The main processes considered in this thesis for creating karst porosity in hydrocarbon karst plays are meteoric karst and hypogene karstification. *Meteoric karst* describes karst where meteoric water provides the main dissolutional fluid for karstification, either by direct rainwater in contact with susceptible outcrops (autochthonous) or by drainage from groundwater flow or streams entering from non-karst rocks (allochthonous) (Ford & Williams, 2007). Papers 1, 2, and 3 deal with different aspects of meteoric karst and Fig. 2 shows examples of karst caves from Northern Norway. *Hypogene* karst comprises dissolution by hydrothermal water and sulphuric acids (Palmer, 2011). It is described by karstification by dissolutional fluids from underground sources, either groundwater heated from the deeper earth crust, or acids entering aquifers (Klimchouk, 2018). Paper 1 discusses the possibility for hypogene karst in connection with a large karst cave, and Paper 3 discusses both meteoric karst and aspects of hypogene karst on- and offshore Norway.

Regarding porosity, it needs to be noted that the primary porosity in carbonates is defined to be related to depositional processes, while secondary porosity is related to open fractures and joints, and tertiary porosity is related to karst. Fig. 3 shows how large karst forms may become– illustrated the large collapse dolina Red lake in Croatia, with a depth of more than 540 m and width of more than 500 m, see also Bonacci *et al.* (2014). Other large-scale karst landforms can be seen in Figs. 2 and 3 in Paper 2.

Figure 2 Karst caves in A: Beiarn in Nordland and B: Salangen in Troms, indicating high porosity/permeability, and in B, the development of conjugated fracture sets. Photos: Terje Solbakk

Carbonates and other karstifiable rocks in Norway and on the Norwegian Continental Shelf

Carbonates are extensively described in Paper 1 in the "Introduction" section, in Paper 2 in the section "Seismic imaging of karst morphology and isomorphs" and in Paper 3 in the section "Karstifiable rocks". The most important observations on carbonates are summarized in the following:

- Carbonates are sedimentary rocks, mainly deposited in the marine environment, but freshwater and open-air carbonates (travertine) are also found (Lucia, 2007).

- Most onshore karst rocks in Norway are meta-limestones found in Early Paleozoic Caledonian nappes (Nakrem & Worsley, 2006), although Permian carbonates are found in the Oslo Graben (Larsen *et al.*, 2006), and Paleoproterozoic carbonates are found in Northern Norway (Nordgulen & Andresen, 2006).
- In contrast on the offshore Norwegian Continental Shelf (NCS), most carbonates are encountered in Late Mesozoic to Early Cenozoic strata, mainly as chalk (in the North Sea) but some Late Paleozoic carbonate strata are occasionally found throughout the entire NCS. Older limestones are rarely targeted for exploration drilling, due to their location at large depths or low hydrocarbon prospectivity, but some wells have proven meta-limestone, e.g. 25/11-1 (see well description at Factpages.npd.no) .

A comprehensive sketch of karst system elements modified from Ford & Williams (2007) and adapted to the Norwegian setting is presented in Fig. 4A (same as Fig. 2A in Paper 3). It illustrates that karst is often broadly divided into active karst (e.g. caves under development), fossil karst (e.g. caves formed as part of an active karst system, but abandoned by present waterways), relict karst (caves with no connection to present-day hydrological regime) and paleokarst as e.g. caves developed with no connection to present-day hydrological regime or landscape (Ford, 1995). However, erosive cycles may rejuvenate fossil-, relict- and paleokarst. Thus, karst caves in the mentioned categories may change regime over time, e.g. paleokarst voids may be opened for new karstification.

Paleokarst is reported from all over the world, see, e.g., Osborne (2000). Ford & Williams (2007) define paleokarst as karst that is hydrologically decoupled from the contemporary system. Paleokarst is often regarded giving the main reservoir porosity of karstified carbonates in submerged settings, due to the de-coupling from the presumed time of karstification (e.g. Loucks, 1999 and references therein). Paleokarst must not to be confused with the term fossil karst, also referred to as relict karst, a type of karst that is decoupled for a relatively short (10-1000s of years) period from the present-day hydrological regime. Decoupling from shallower passages in an active cave system may occur due to valley lowering, an effect of topographic changes caused by glacial cycles (Lauritzen, 1986; Skoglund *et al.,* 2010). Short-term geological changes may connect these fossil karst conduits back into the present hydrologic regime.

Deep weathering surfaces and paleo-surface landforms may bear a resemblance to karst (Ford & Williams, 2007, Halliday, 2007). This leads to the next term, "pseudokarst", that is often used to describe karst-like features; mainly cave-like landforms such as open lava tubes, piping features in unconsolidated fine-grained sediments and, for silicate formations, pseudokarst can be created by arenization of porous quartzites (Wray & Sauro, 2017;

Halliday, 2007). Arenization describes the process of quartz dissolution and porosity evolution in pure quartz sandstones and meta-quartzites, according to definition given in Wray & Sauro (2017).

Figure 3 Karst landforms can reach extreme sizes, like this collapse dolina in Imotski, Croatia, with a surveyed depth of more than 540 m and more than a 500 m width (Bonacci et al.*, 2014). Note arrow to person for scale in upper left corner. Photo mosaic (Brenizer method): Terje Solbakk.*

Marine abrasion may create karren-like patterns on marine platforms, and abrasion caves also resembles karst caves (see Paper 3: Table 1).

Background of offshore and onshore karst exploration in Norway

In the past decade, hydrocarbon discoveries have been made in new plays with karst porosity on the NCS. With the discovery wells 7120/3-1 'Gohta' and 7220/11-1 'Alta' in the southwestern Barents Sea, moveable oil and gas have been proven in reservoir rocks with good tertiary porosity from karst dissolution (press releases at www.npd.no).

Cave conduits are reported as penetrated from exploration drilling on the NCS, e.g., in the appraisal well 7220/11-3 in the 'Alta' discovery (Barents Sea) and in the well 16/1-2 at the Utsira High (North Sea) (factpages.npd.no). The submerged karst of the Norwegian Continental Shelf should, in fact, be referred to as paleokarst (Osborne, 2013), meaning karst hydrologically decoupled from the contemporary system (Ford & Williams, 2007). The exception being possible on-going hypogene karstification near rift margins, as discussed in Paper 3.

The submerged Loppa High in the Barents Sea (Larssen *et al.* 2002; Smelror *et al.* 2009; Stemmerik *et al.* 1999; Stemmerik and Worsley 2005), has a relatively large amount of accessible data in the form of well logs, well cores and relatively good seismic coverage and there are published several scientific papers and conference presentations on the area (Ahlborn *et al.*, 2014; Hunt *et al.*, 2003; Hunt *et al.* 2010; Kovacova, 2010; Sayago *et al.*, 2012, Sayago *et al.* 2018, Svånå, 2013).

Furthermore, in the North Sea, karst features have been identified in wells at the Utsira High in Zechstein carbonates, and within and beneath the Johan Sverdrup field (wells 16/3-5, 3-7 and 3-8, Sorento *et al.*, 2018). However, the karst porosity has been destroyed by diagenesis in the hydrocarbon filled part, thus not adding to the reservoir porosity. A handful of other exploration wells both in the North Sea and the Norwegian Sea show karst features but have not generated any economic result – table 3 in Paper 3 provides an overview.

Karst landforms in Norway are common (Horn, 1947; Corbel, 1957; Lauritzen, 2010; Korneliussen *et al.*, 2013). Karst caves with a length of more than a few tens of meters are reported from all regions in Norway, including Svalbard (Lauritzen, 2001; Lauritzen, 2010; www.speleo.no). Most of these caves are developed within Caledonian nappe marbles, and the age of the karstification is mainly found to be Late-Quaternary. However, the karstification generally developed in concert with repeated glacial/interglacial cycles (Lauritzen, 1986). Glacial erosion had a devastating effect on former karstified landscapes, strongly reducing the survival rate of older caves. The existence of older caves that have been reworked is indicated by Uranium-Thorium series dating of speleothems (secondary deposition of minerals in caves) that revealed Mid-Quaternary ages, and even older pre-Quaternary ages were suggested for some caves (Haugane & Grønlie, 1988; Lauritzen, 1990; Lauritzen, 2008).

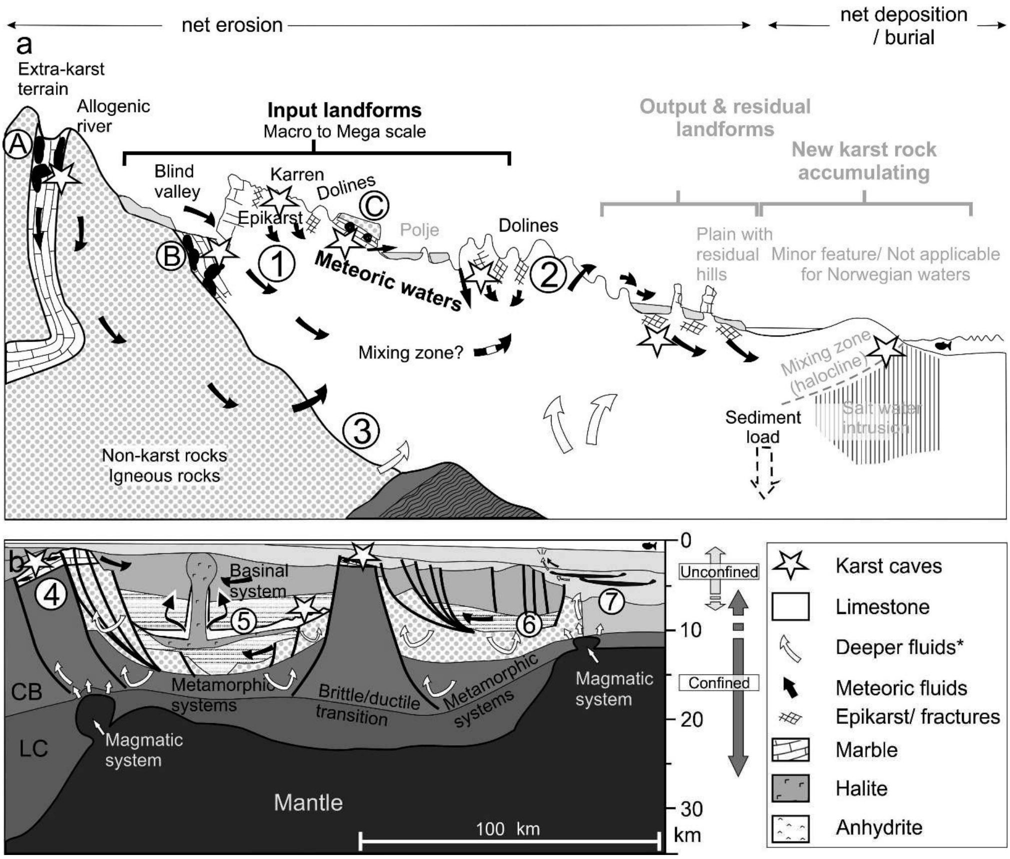

*Figure 4 Comprehensive karst model, modified from Ford & Williams (2007) and adapted for the Norwegian onshore conditions, with arrows indicating potential fluid routes. Figure a): Onshore karst model, showing strongly folded Caledonian nappes and meta-carbonates of Norway sub-vertical setting (A), perched setting (B) and confined setting (C). Numbers refer to examples for karstification with different fluid sources from Norwegian mainland and offshore areas. Typical cave settings generated by meteoric waters (1); mixing zones of meteoric and basinal fluids (2); pure hypogenic setting, as reported from Oslo graben area (Lauritzen and Dahlgren, 2017)(3); figure b) hypothetic offshore settings derived by transferring predominant onshore Norwegian karst landscapes to the offshore utilizing Norwegian exploration wells. Idealized setting mimicking the Loppa High with meteoric and hypogene fluids (metamorphic and magmatic) (4); a basinal system with salt domes (5); outer margin rift basin (6); continent-ocean transition zone with magmatic systems (7). The section in figure b is sketched after Faleide et al. (2008).*Deeper fluids includes both basinal fluids and fluids from the lower crust/mantle.*

Overview of the geological setting of rocks in Norway

Norway, including its continental shelf area, is situated in the northwest corner of the Eurasian plate and part of a passive margin (Martinsen & Nøttvedt, 2006).

Quaternary glacial and earlier erosion has exposed crystalline rocks of Paleozoic and older ages on land, with only minor exceptions of younger rocks preserved in inlier basins (Bøe *et al.*, 2010). Glacial erosional products were loaded onto the nearby shelf areas (Hughes *et al.*, 2015). Further back in time, structuring due to various episodes of plate tectonic extension and compression since the Archean Eon and with focus at different locations, dissected onshore and offshore areas, dividing them into a multitude of structural elements separated by small and large fault systems, as shown in Fig. 4 (Faleide *et al.*, 2015).

The following overview is based on different chapters in Ramberg *et al.* (2006) summarizing how the Norwegian bedrock witnesses a complex history with several periods of orogenesis, continental break-ups, and sedimentation. The oldest rocks being part of the Fennoscandian shield and comprising Archean crust (aged older than 2500 Ma) exposed in the northernmost part, are referred to as greenstone. These are found together with an overlying Paleo-Proterozoic sequence, layered mafic intrusions, mafic dykes, and meta-sedimentary rocks. Two orogenies are identified from Paleoproterozoic (1600-2500Ma) in this region; the Svecokarelian (from the Siderian to Orosirian Periods) and Svecofennian orogeny (from the Orosirian to Statherian Periods). The rocks were subsequently intruded by large granitic plutonic rocks of mainly Statherian age forming the Trans-Scandinavian Intrusive Belt (TIB).

Proterozoic rocks of Calymmian to Tonian age (c. 720-1600 Ma) are found in the southwest of Norway, comprising an approximately 800-million-year long period with a plentitude of volcanic, magmatic and sedimentary rocks deposited, deformed and metamorphosed mainly during the Gothian (c. 1500-1750 Ma) and the Sveconorwegian orogeny (c. 970-1130 Ma). Later break-up of the Rhodinian supercontinent during the Tonian led to the establishment of the continental plate Baltica. Along the margin of Baltica's northwestern margin, km-thick deposits of coastal plains, shallow marine and deep marine sediments were deposited in basins throughout this period in a varying climate. The thick sediment package deposited here is referred to as Sparagmite and is encountered over large areas in northeastern, southern, and western Norway.

Plate compression during the Late Cambrian (c. 485-541 Ma) lead to oceanic plate subduction in the Iapetus ocean and generated several volcanic island arcs, both along the Baltica margin and along the Laurentia margin followed by island arc collisions. This is regarded as the precursor of the Caledonian orogeny, a continent-continent collision between Laurentia and Baltica starting in the Lower Ordovician and continuing until the Devonian, stacking rocks of island arc and oceanic crust onto Baltica. At the same time, island arc collision on the opposite (Laurentian) side led to subduction along the Laurentian margin continuing into the Middle Ordovician, where nappes of volcanic arc origin together with ocean crust were transported and stacked onto Laurentia.

The Early Silurian (Llandovery Epoch) saw the development of new volcanic island arc systems along Laurentia, with a new mid-ocean ridge along the Laurentian margin. This led to a second island arc system collision with Baltica, being stacked onto the continental plate, with a subduction phase on the Baltic continental margin during Wenlock times. The Caledonian orogeny ended with a complete continent-continent collision with several nappes (thrust packages) constituting the Caledonian mountain chain being stacked onto the Baltic shield in the Late Silurian (Ludlow-Pridoli)- Early Devonian, often referred to as the Scandian phase. Caledonian nappes are generally divided into four allochthons, from proximal to distal (Baltic to Laurentian) origin.

Later extension and collapse of the Caledonian mountain chain led to erosion and infilling of thick intra-montane basins during the Lower to Upper Devonian. Carboniferous and Permian rocks are generally not preserved on the Norwegian mainland, with the exception of the Late Carboniferous- Early Triassic rifting phase of the Oslo Graben. Neither are the later Mesozoic/Cenozoic rocks preserved onshore Norway. The only exception is a small Mesozoic graben at Andøya, Northern Norway. Some submerged inlier basins with Mesozoic sediments are preserved on the Norwegian strandflat and inner fiords (Bøe *et al.*, 2010). Subsequent massive erosion is mostly attributed to Pliocene and Pleistocene glacial activity, but also Tertiary erosion. The youngest volcanic activity evident onshore Norway is related to Early Permian dyke intrusions.

Analytical methods

This section describes the geophysical methods and field work that forms the basis for the thesis work. Geophysical methods for hydrocarbon exploration are commonly used on the Norwegian Continental Shelf (NCS), mainly 2D and 3D reflection seismic, but also Electromagnetic methods (EM) are emerging as an important tool for hydrocarbon prospect evaluation. Regional (third-party) gravity and magnetic data are also commonly used, mostly in basin scale evaluations (cf. Landrø & Amundsen, 2018). Methods for karst exploration are also summarized in Fig. 1. Geophysical data used in this thesis are the candidates own microgravimetric data used for modelling purposes, and available seismic imaging data used for interpretation purposes.

Fieldwork

Paper 1 reports field data gathered during the autumn of 2007 in Fauske, Nordland, in cooperation with Stein-Erik Lauritzen (SEL) (University of Bergen), Walter Wheeler (Unifob/Norce) and the late Arne Gidskehaug (University of Bergen). Field data gathered included gravimetry and dGPS data (Fig.5).

Figure 5 Glimpses of fieldwork during field season 2007. A: Kjetil Broberg next to the dGPS total station at the Svarthammar plateau. B: Terje Solbakk reading the Lacoste&Romberg gravimeter. C: Terje Solbakk mounting gear for cave profile surveying. Photos: A: Terje Solbakk, B and C: Kjetil Broberg.

A field visit in September 2017 on the Makarska coast in Croatia involved visits to large-scale karst landscapes that provided data input for Fig. 3.

The candidate participated as trip leader on two karst themed excursions for Lundin Norway AS, one to Verdal in Trøndelag and one to Fauske, Nordland, and as a co-leader on one excursion for Aker BP in cooperation with Arne Grønlie. In addition, one field day was held in cooperation with NGU at the Tromsdalen limestone quarry in Verdal in April 2019 to sample karst infill sediments (see appendix A2).

Gravimetry

Gravity field surveys, cf. Dentith & Mudge (2014), address the interaction of objects separated by a specific distance through analysis of the gravity fields surrounding each object. The gravity field is explained in terms of mass, density and the gravity equation. Mass refers to the amount of matter in an object, while density is the mass contained in a unit volume of the matter, where:

$$Density = \frac{\text{mass}}{\text{volume}} \quad \text{or} \quad Mass = density \text{ x } volume$$

The gravity equation describes how objects attract each other according to Isaac Newton's universal law of gravitation with a force proportional to their masses. The attractive force (F) between to masses (object m1 and m2), separated by a distance (r), with the universal constant of gravitation G= 6.67430×10^{-11} $N \cdot m^2/kg^2$ is described:

$$F = G\frac{m1\, m2}{r^2}$$

Thus, the attractive force acting on an object at sea level on the Earth gives an approximate acceleration of 9.81 m/s^2 and should ideally be the same all over the planet for any object of any mass at the sea level. However, due to a heterogeneous subsurface, the Earth's rotation and lateral variations in the Earth's radius at sea level, significant variations occur in this acceleration value, which also varies with topographic height. Although these changes are very small in comparison with the average strength of the Earth's gravity field, by measuring small differences, one can invert gravity field measurements to detect small changes in subsurface densities. The common unit used for gravity acceleration is the gal, where 1 gal = 1 cm/s^2. Gravity field measurements are now so accurate that values of 10^{-3} gal (=mgal) down to 10^{-6} gal (=microgal) are common.

Air- or water-filled caves give a major density contrast to the surrounding bedrock which will result in a gravity anomaly (Chico, 1964; Butler, 1984; Styles *et al.,* 2005; Kaufman and Romanov, 2009; Kaufmann *et al.,* 2015; Martinez-Moreno *et al.,* 2014; Martinez-Moreno *et al.,* 2015; Braitenberg *et al.,* 2016). For offshore exploration this method may be of advantage in identifying larger areas of submerged karstified rocks, due to the decay characteristics of the gravity field with increasing depth of the target, see Paper 1. The candidate applied this method to an onshore cave in Fauske, Nordland, Northern Norway (Lauritzen *et al.,* 2005). A fieldwork campaign with gravity measurements was conducted during the late autumn of 2007 at the Mefjell massif on the northeast side of the plateau above the Svarthammarhola Cave (SHC), covering an area of approximately 280 x 300 m (Figs. 3 & 7 in Paper 1). The station grid was designed to cover parts of the biggest cave chamber of the SHC, and an area where cave surveying and visual inspection on the land surface revealed the possibility of a cave continuation in an easterly direction.

Gravity data were acquired using a LaCoste&Romberg Model D gravimeter. Each gravity measurement was positioned with a Topcon differential L1-L2 GPS-GLONASS system to create a local digital elevation grid model with an approximate (20 x 20 m) cell size. For further details please see method section in Paper 1.

Seismic

Seismic methods uses elastic waves to image and interpret the subsurface, cf. Dentith & Mudge (2014), or Landrø & Amundsen (2018). These waves are generated by an accoustic source (e.g. a marine air gun or mechanical vibrator) and propagate through the subsurface. There are two main seismic waves; body waves and surface waves. Body waves are divided into two types; longitudinal with P- (primary) waves and transverse with S- (secondary) waves. Surface waves are divided into three main types; Rayleigh (ground-roll) waves, Love (shear) waves and Stoneley (tube) waves. Here, P waves are used where it is the velocities and elastic properties of different rocks, lithological boundaries, structural features or fluid interfaces, that reflect or refract the seismic waves, thus creating different seismic wave paths. Receivers, geophones on land or hydrophones on sea, record the different seismic waves travelling different paths to the subsurface. On the NCS, seismic reflection surveys are commonly used on all scales from basin to hydrocarbon prospect evaluation, cf., Landrø & Amundsen (2018).

Karstified reservoirs should therefore be theoretically identifiable on 2D and 3D seismic reflection data, due to the karst cavities within the rock mass providing huge, sharp, negative impedance and density contrasts, as exemplified in Fig. 1 in Paper 2. To compare, a sandstone – shale boundary would give a moderate, low impedance contrast, with a negative polarity. Karst interpreted from seismic data is reported by several authors, e.g. Ahlborn *et al.* (2014), Bourdon *et al.* (2004), Fournillon *et al.* (2017); Hunt *et al.* (2003), Sayago *et al.* (2012), Sayago *et al.* (2014); Sayago *et al.* (2018); Tian *et al.* (2016), Vahrenkamp *et al.* (2004), Xu *et al.* (2016); Yu *et al.* (2018) and Zeng *et al.* (2011). Analogues for submerged karstified reservoir rocks are easily accessible around the world, also in the Arctic area, e.g., Eliassen & Talbot (2005), Smith *et al.* (1999) and Stemmerik & Worsley (2005). In this thesis work, 2D and 3D seismic data were available for seismic interpretation in offshore areas. Seismic reflection data available through the Diskos database were imported into an in-house Petrel workstation (Schlumberger) for seismic interpretation. Newer, proprietary 3D seismic data (owned by production license holders on the Norwegian Continental Barents Sea Shelf) became available through industry partners in the project funded by the ARCEx Research Centre. For further details please see chapter on Seismic interpretation in Paper 2.

Well data

There are several common well tools that gather different physical properties through the borehole walls, see Al-Marzouqi *et al.* (2010) for an overview of such logging tools used when exploring carbonate reservoirs. Well logs from all released wells are available through the Diskos database provided by the Norwegian Petroleum Directorate(NPD). Several boreholes penetrate the Upper Paleozoic carbonates of the Loppa High. A plethora of data is available from the Norwegian Petroleum Directorate Factpages (factpages.npd.no) on exploration, production, and scientific drilling wells (named IKU-wells, available through sintef.no), from press releases to company completion reports. This wealth of data is made use of in Papers 2 and 3.

Studies of offshore well cores have been undertaken at Norwegian Petroleum Directorate's core store in Stavanger during spring 2015, where core samples were taken for thin section preparation and analyzes by microscopy. Results were correlated with seismic interpretations (Paper 2) and porosity estimation (Paper 3).

Research methodology

Gravity data processing and modelling (Paper 1)

The gravity data was processed using Microsoft Excel spread sheets following the workflow displayed in Fig. 6 (see Paper 1 for details)

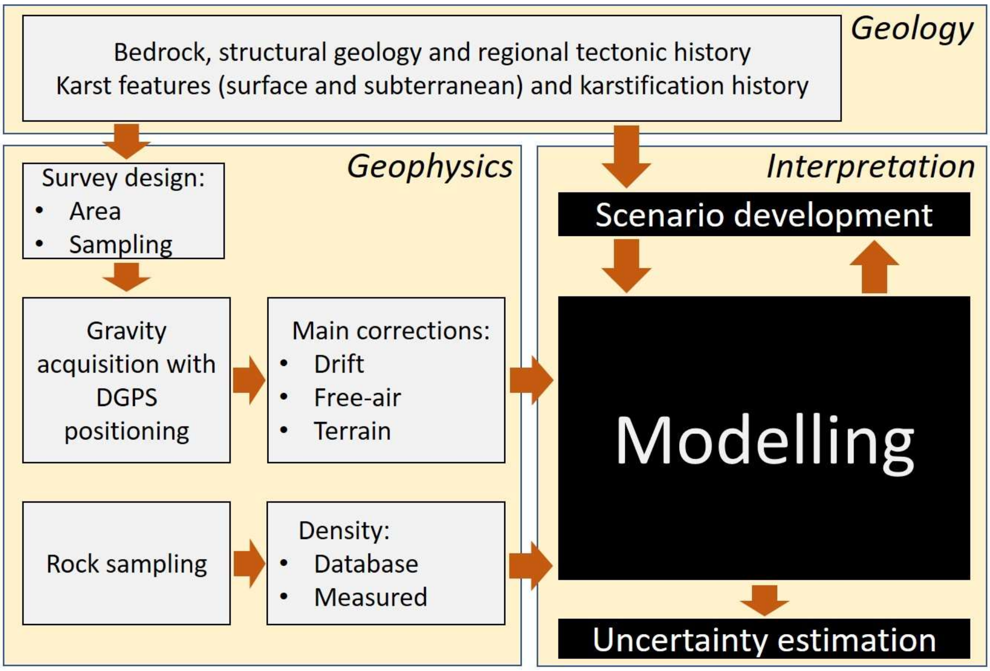

Figure 6 A workflow for gravity exploration of cave passages (Fig. 12 in Paper 1).

Altogether, the measurement error is estimated to be ± 0.2 mGal (see Table 2 in Paper 1). All measurements are kept as relative gravity values and have not been corrected to absolute gravity values. This approach is common for microgravimetry studies (Ardestani, 2008; Beres *et al.*, 2001). Note that microgravity studies deal with local density changes within a rock mass and cover a small areal extent, addressing targets usually detectable within a milli- to microgal range.

Terrain correction was performed with software Modelvision (version 15, Tensor Research). The terrain model was constructed by converting the terrain into a body faceting the terrain surface. The facets used were small in size within the study area and larger in the framing region of the study area. DGPS measurements provided the topography for the study area, whereas a digital elevation model (DEM) was used outside the study area.

The software Modelvision was used to construct the density model formed to represent the cave and its surrounding rocks in a way that resembles the measured gravity anomalies. Modelvision software builds the geometry of the subsurface by inserting bodies of different shapes into the subsurface volume. The bodies' densities, as well as the background density for the subsurface, need to be set by the user. All bodies within the subsurface contribute to the gravity anomalies. This framework defines a 3D environment with 3D bodies. Body geometries can be modified in vertical profiles or in the map plane. Here the following body types were used:

- Horizontal prisms; defined by its polygonal cross section in profile and/or map view, where strike angle, strike lengths and plunge can be modified.
- Frustums; with their top and bottom defined by topographic surfaces in the map plane.

It was challenging to transfer the geometry of the known cave, as described by speleological terms, into a format that could be read by Modelvision. In order to create the density model of the known cave, its cave ceiling and cave floor were exported from the Grottolf Software (Lauritzen, 2006), imported into the Petrel software (Schlumberger), and exported to Modelvision as grid surfaces. After calculating the gravity anomaly of the known cave and comparing these gravity values with the measured gravity, a misfit was observed, which clearly indicated that additional shallow cave rooms were needed. Subsequently, further bodies were created with densities that differ from the background density in order to achieve a match between modeled and measured gravity anomalies, as well as to honor the observed geological features and lithology in a geologically realistic way. The workflow for the data collection, processing, and modelling is summarized in Fig. 6 (Paper 1: Fig. 12).

Seismic interpretation (Paper 2)

Seismic interpretation was performed using a Petrel workstation environment (Schlumberger), and surface maps, thickness maps and attribute maps were produced from interpreted seismic horizons. Subsequently, faults were mapped out from seismic discontinuities and finally, the unconformities that were needed to interpret the target zone (Paleozoic carbonates). The work was focused on unconformities (Fig. 6 in Paper 2) that were associated with karst topography as known from literature (see below and Paper 2). Focus areas were chosen after the criterion that geometries could be associated with karst or karst-like features along these surfaces.

Selected well log data from the Loppa High were imported into the Petrel workstation (Schlumberger), visually inspected and used for lithostratigraphic to seismic correlation by means of wireline logs. Information and data from the wells are available from the Norwegian Petroleum Directorate's Factpages (www.factpages.npd.no, visited May 2016 – September 2019).

Assessment of preexisting knowledge, GIS and microscopy (Paper 3)

Paper 3's comprehensive objectives required assembling all existing information on karst with the regional scope to predict the hitherto unknown karst potential. This required creative solutions to find existing knowledge. A comprehensive literature research has been performed both on the Norwegian continental shelf and elsewhere in the world, as well as an assessment of non-published information by personal contacts. Generic reports on karst from offshore exploration wells are commonly found in well drilling result press releases from the NPD's Factpages. Additional information can be obtained from older wells after a two-year publishing lag on data from drilling completion date, in case the well is "dry" or if no commercial exploitable hydrocarbons were encountered. This publishing lag increases to 20 years if a hydrocarbon discovery is made in the well. The extent of the available drill data may vary, but in, e.g., completion reports and logs, notes on karst features (larger vugs, dissolutional features associated with unconformities/paleosols et cetera or other observations) are commonly noted, as there are systematic guidance schemes for well loggers to follow. During the publishing lag time, conference presentations may reveal more data on possible karst properties encountered in exploration wells. No systematic approach can be expected here. The well data presented in this article are gathered mainly from NPD Factpages. Scientific well drilling (SINTEF IKU wells), onshore information and seismic interpretations (see subchapters on sea areas in Paper 3) may also add information on potential karst offshore. Scientific articles may also contain information on this matter.

GIS tools (ArcMap 10.7) were used for data compilation – both map data as well as information from karstification. Topographic data sets are freely available for download from the Norwegian mapping authorities (Statens kartverk – www.kartverket.no), the Norwegian Petroleum Directorate (NPD) - www.factpages.npd.no, and the Norwegian Geological Survey (NGU – www.ngu.no). Most of these data sets were downloaded from www.norgedigitalt.no. From the NPD, several other data sets were available from the NCS, such as hydrocarbon fields and discoveries, structural elements, faults, and lineaments.

Several cores from selected exploration wells were logged at NPD's Core store. Exploration well 6608/8-1 (Fig. 1, Paper 3) was sampled for thin section preparation based on well description report from NPD's www.factpages.npd.no. Existing thin sections with carbonate lithology at the NPD have been inspected, and a selection from the Barents Sea area has been taken out for further work. The thin sections were closer examined with transmitted light microscopy (Fig 5 and 10 in Paper 3) at the NTNU IGP thin section lab. Porosity analysis was done digitally with open-source software ImageJ available with Fiji distribution (Schindelin *et al.*, 2012) on these thin sections (see Fig. 10 in Paper 3).

Manuscripts objectives and author contributions

Paper 1 – Detecting multiscale karst […]

Detecting multiscale karst features including hidden caves using microgravimetry in a Caledonian nappe setting: Mefjell massif, Norway

Norwegian Journal of Geology. Published online 20. November 2018.
https://dx.doi.org/10.17850/njg98-3-04

Main objectives of the paper:

1. *To investigate with the gravimetric method a possible continuation of a very large karst cave passage situated within Caledonian metasediments, where the cave passage continuation is indicated by collapse sediment infill on the surface or within the known cave*
2. *Provide a workflow applicable for mapping near surface karst caves by microgravimetry*

Candidate's Contributions: My contribution to this article was data acquisition in the field (2007), data processing, modelling, interpretation and writing the manuscript. My co-supervisor Christine Fichler contributed by scientific discussion on the gravity interpretation and helped with editing of the manuscript. My main supervisor Philip Ringrose contributed with scientific discussion and refinement of the manuscript. Co-author Walter Wheeler (Unifob/Norce, Bergen) participated in field work (2007) and contributed to the subchapter on dGPS data and refinement of the manuscript. Field data from co-author Stein-Erik Lauritzen's (University of Bergen) Svarthammar project (Lauritzen et al., 2005) was incorporated in the manuscript, and he also assisted in editing. The gravimetry data collection was based on an original idea by Lauritzen and Wheeler. The article is published in an open access journal:

Geological Society of Norway

Detecting multiscale karst features including hidden caves using microgravimetry in a Caledonian nappe setting: Mefjell massif, Norway

Terje Solbakk[1], Christine Fichler[1], Walter Wheeler[2], Stein-Erik Lauritzen[3] & Philip Ringrose[1]

[1]*Department of Geoscience and Petroleum, Norwegian University of Science and Technology (NTNU), Sem Sælands veg 1, 7491, Trondheim, Norway.*
[2]*Uni Research CIPR, Nygårdsgaten 112, 5007 Bergen, Norway*
[3]*Department of Earth Science, University of Bergen, Allégaten 41, 5007 Bergen, Norway.*

E-mail corresponding author (Terje Solbakk): terje.solbakk@ntnu.no

Cave passages and karst features form negative density contrasts expressed in gravity field anomalies. We present an interpretation approach for microgravimetry, applicable for challenging geological settings with heterogeneous lithologies. The workflow covers not only detection of large cave rooms, but also deals with minor karst features (epikarst) in carbonate rocks. Challenges due to heterogeneous infill of large cavities and variations in carbonate facies are addressed. We used 3D forward modelling of surface gravity measurements to investigate a large karst cave complex, known as the Svarthammarhola cave, in the Caledonian nappe setting of Nordland. The most important result relates to distinct gravity lows detected in the survey, which are interpreted as hitherto unknown and inaccessible cave rooms, some of them of a very large size. These correspond with known collapse and sediment infill features both at the surface and inside the Svarthammarhola cave system. This expands the known cave in an eastward and northward direction.

Combining the cave's position at the top of the hinge of a large antiform where we also modelled uncommonly high densities, together with the cave's outstanding size, opens for new interpretations of the speleogenesis of the Svarthammarhola cave. The study also has wider implications on how gravity field data can be used for the understanding of complex subsurface karst features.

Keywords: gravity acquisition, gravity interpretation, cave detection, microgravity, karst

Received 12. February 2018 / Accepted 7. July 2018 / Published online 20. November 2018

Introduction

Karst describes a suite of surface and subsurface landforms developed through chemical dissolution of soluble bedrock, of which carbonates are the commonest. Dissolution increases the amount of secondary porosity of the rock mass on a wide range of scales, leading to a decrease of surface drainage, underground caves, streams and sinks, springs and surface expressions characterised by undermining, forming dolines of various kind. Further evolution may lead to extensive collapses and disjunction from the contemporary hydrological system, forming paleokarst. 'Karst porosity' is therefore a combination of chemical (dissolution) and mechanical (collapse) processes. The karst terms used here refer to the textbook of Ford & Williams (2007). Dolines, in a larger sense, can be related to collapse, sag and subsidence by chemical and/or mechanical breakdown. Epikarst describes the weathered and fractured three to ten uppermost metres of the karstified rock, and its characteristics may vary extensively (Ford & Williams, 2007). Although the epikarst zone often has a scattered distribution, epikarst can be found over several square kilometres in lateral

Solbakk, T., Fichler, C., Wheeler, W., Lauritzen, S.-E. & Ringrose, P. 2018: Detecting multiscale karst features including hidden caves using micro-gravimetry in a Caledonian nappe setting: Mefjell massif, Norway. *Norwegian Journal of Geology 98*, 359–378.
https://dx.doi.org/10.17850/njg98-3-04.

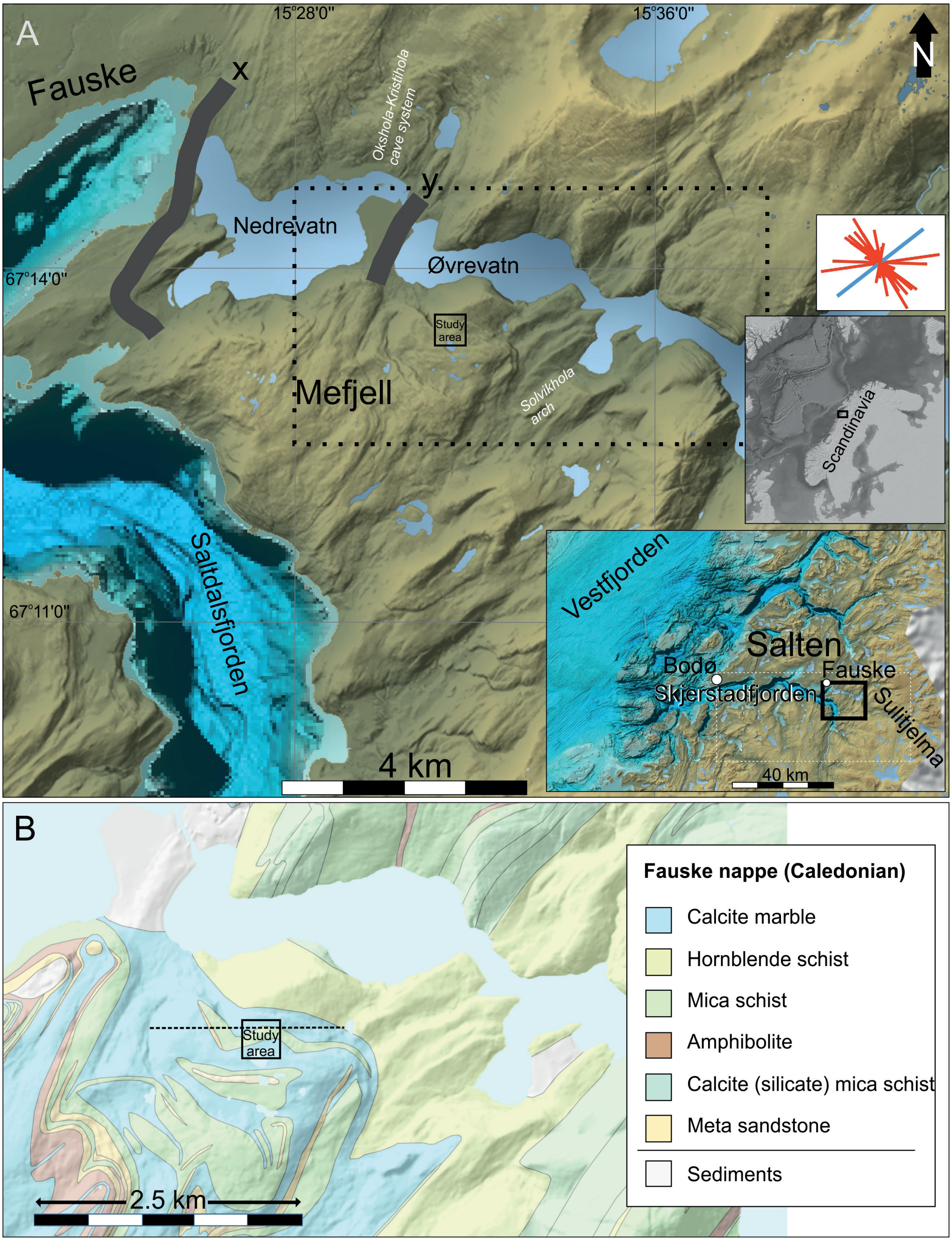

Figure 1. (A) Topographic map of the greater Mefjell massif with 'Study area' shown in detail in Fig. 4, (www.kartverket.no, accessed 01.02.2018). Stippled box marks location of the geological map shown in (B), features X and Y are end moraines (Andersen, 1975). Main lineament trends (red, in the inset, top right) interpreted from topography map within the (B) frame, with main foliation trend (blue) derived from the geological map in (B), with normalised trend line length. (B) Geological map; the stippled line refers to Fig. 15B.

extension. In a glaciated setting, the epikarst zone may be complete or partly removed.

We look closer into the area around the Svarthammarhola cave (SHC), located in the Mefjell massif of Nordland, northern Norway (Fig. 1A), which is the largest cave volume found in Scandinavia as described below in more detail. In our study area we encounter typical large-scale (more than a few metres width and height) karst landforms such as caves, dolines and epikarst.

Caves can be accessible to man, and surveyed by means of compass, clinometer and distance tools of different kinds. These data usually just document the existence of, and provide some basic information about the caves, but do not necessarily give details of all existing cave rooms or geological features within the cave and rock mass. However, human exploration is strongly biased; a cave map is always a minimum estimate of the void porosity. Indications of hidden, inaccessible cave passages can be deduced from cave surveying and inspection. Examples include: descriptions of rock shelters with collapsed back wall next to known cave systems, sag depressions on the land surface above the cave, choked dolines or vertical pipes, and sediment-choked passages or water-filled passages. However, an estimate of the extension and geometry of hidden cave rooms requires either physically entering the cave system or by using remote geophysical mapping methods, as described here.

The subsurface density is directly expressed in gravity data, and therefore gravimetric exploration can be a valuable method for detection of karst porosity and hidden caves. The main challenge for gravimetric mapping of karstified rock formations is that the changes in density occur over a wide range of scales due to the chemical dissolution process and the complexity created by subsequent infill (by air, water or sediment).

Several papers have demonstrated the use of gravity measurements as an aid to find natural and manmade cavities; either as a standalone method, or combined with other geophysical methods, or by invasive techniques such as drilling or entering the cave. Chico (1964) was the first to go into detail on detection of caves by gravimetry, and referred to earlier work pointing to such possibilities. Later, Butler (1984), Barrows & Fett (1985), Styles et al. (2005), Ardestani (2008), Martinez-Moreno et al. (2014), Braitenberg et al. (2016) and Kaufmann et al. (2015) showed examples of successfully detecting karst caves, some supported also by other geophysical methods like resistivity imaging and self-potential surveying (Kaufmann et al., 2015) or by drilling (Barrows & Fett, 1985; Ardestani, 2008). However, at times, inconclusive results were reported due to the inherent ambiguity in gravimetric exploration; for example, Kaufmann & Romanov (2009) described a case where the gravimetry data could not distinguish between a buried doline and a cave. Epikarst has generally not been considered in earlier work applying gravity data to karst cave exploration.

To our knowledge, gravity measurements have not been used for karst cave exploration in Norway, and the results should therefore be of value to understanding the local karstic geology as well as buried karst systems in general. The SHC provides an excellent opportunity to explore a large cave system on all scales.

Fig. 2 shows the amplitude of the gravity anomaly of an open sphere and a horizontal cylinder within a rock mass, calculated with formulas from Chico (1964), demonstrating that the gravity response decreases with depth. A cylinder at a depth of 250 m produces only a 1/100th of the anomaly produced if at a depth of 10 m, documenting that the most dominant anomalies relate to sources in the uppermost subsurface. The depth of the SHC, marked in Fig. 2, indicates that a cave room with the size of the SHC should be detectable more than some tens of metres below the surface. Another effect of an increasingly greater depth down to the void is an increasing wavelength. The SHC is positioned at a depth where the details of the cave passage geometry disappear into smooth long-wavelength anomalies. This indicates that shallower cave rooms, if they exist, will dominate the gravity signal. A further challenge is that the gravity signal of the cave room is superimposed on the gravity signal from host-rock heterogeneities.

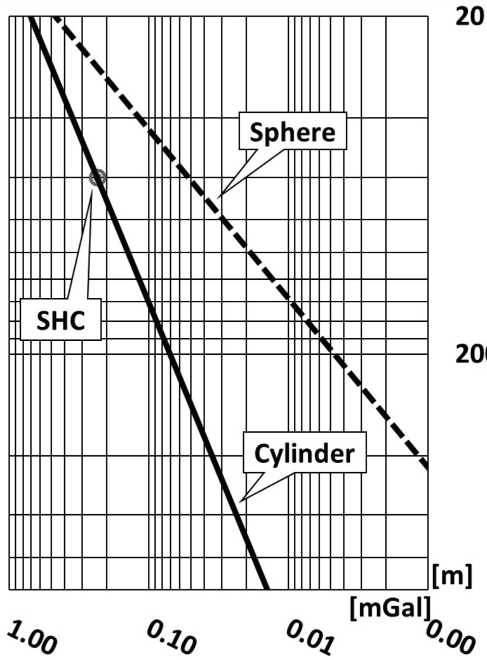

Figure 2. The modelled maximal gravity anomaly size of a sphere (dashed line) and a horizontal cylinder, both with a radius of 20 metres, buried at various depths with density contrast 2770 kg/m^3. Y-axis shows depth to centre of sphere/cylinder. Known cave indicated (red circle). SHC – Svarthammarhola cave.

The aim of this paper is to use microgravimetry to investigate the geometry of hidden cave passages believed to be a continuation of the SHC, and the distribution of multiscale karst features. This study demonstrates the potential for near-surface mapping and discusses the potential for application in hydrological or petroleum exploration studies. Finally, we discuss implications for the speleogenesis of the SHC.

Geological setting

Regional geology, geomorphology and glacial geology

The bedrock of the central part of Nordland County can be characterised as mainly comprising Caledonian folded metasedimentary rocks (Roberts et al., 2002) of Laurentian origin, resting on older (autochthonous) metasedimentary and crystalline basement rocks. The Caledonian rocks are divided into several nappes, and the Mefjell massif is situated within the Fauske Nappe. This nappe belongs to either the Upper or the Uppermost Allochthon (Drivenes et al., 2016); ages are disputed, but Roberts et al. (2002) argued for an Early Cambrian age. From the topography and bedrock map (www.ngu.no/emne/kartinnsyn accessed 01.02.2018; Fig. 1A, B; Kollung & Gustavson, 1995) the structural setting of the eastern part of the Mefjell massif can be described as mainly comprising a NNE–SSW-trending antiform. The antiform's core is composed of hornblende schist of the Håskolt Formation, and is partly conglomeratic. It is overlain by calcite marble belonging to the Rognan Formation, which again is overlain by, and interfingered with, mica schist of the Langvad Formation of the Pålsfjell Group together with quartzite of the Pothus Formation. Amphibolite is also found interfingering with the mica schist. The Caledonian nappes were transported in an east-southeasterly direction over Proterozoic metamorphosed granitic gneisses (referred to as Krågakomplekset), younger mica schist and meta-arkose. Intrusions of Meso- to early Neoproterozoic plutonic rocks within the nappes, earlier assigned to Cambro–Silurian ages, are also found in the vicinity (Agyei-Dwarko et al., 2012).

The greater Salten area is dominated by a major fjord system, Saltfjorden, incised in an undulating peneplain found at altitudes between ~400 and 1000 m a.s.l. with mountain massifs reaching slightly over 1900 m a.s.l. (Lidmar-Bergstrøm et al., 2007).

The Nordland area was repeatedly glaciated and heavily eroded throughout the Quaternary period (Mangerud, 2004). Quaternary glacial erosion has removed most post-Caledonian rocks and geomorphologically severely modified, enhanced and/or over-deepened the relief leading to an extensive fjord development, glacifluvial canyons and glacially-derived deposits (Fig. 1A; Andersen, 1975). Glaciers still exist some kilometres away from the cave area, but their glacial drainage does not affect the Mefjell massif or bring glacial water into our study area. Several cirque forms can be observed in the topography around and at the Mefjell massif. Evidence for a stagnant ice mass in the SHC area may indicate a relict glacier (see SHC description below for details). Pronounced fjord features and cirques are also developed together with the deposition of large amounts of glacial deposits in the areas of lower elevation. During the last glacial maximum, the general ice movement was towards the NW (Andersen, 1975). Deglaciation led to further development of the relief-controlled ice flow from the remaining ice sheet, following the topographic lows of valleys and fjords. In the vicinity of the cave, two end moraines are recognised along the Nedrevatn/Øvrevatn valley (Fig. 1A): the Finneid and the younger Øvrevann end moraines. These end moraines are assigned to a Pre-Boreal age and thus give a minimum age for ice-free conditions at the cave plateau. A radiocarbon age of 8760 ± 150 years B.P. has been reported for shells found in marine silt and clays overlying the moraine, giving a minimum age for the Finneid end moraine (Andersen, 1975). Shells from assumed contemporary marine layers deposited in front of the Finneid moraine ridge were dated to 9570 ± 150 years B.P.. Thin or scattered sediments cover the study area.

The post-glacial marine limit is modelled to have reached about 150 m above present-day sea level (www.ngu.no/ accessed 01.12.2018) which reaches the elevation of the lowest surveyed passage in the SHC. However, marine sediments have not been observed within the cave. Caves can generally act as sediment traps under glacial conditions, but limited accommodation space and flush episodes by glacial meltwater, or freeze/thaw cycles within the cave, can lead to very scattered sediment packages of uncertain origin (e.g., Valen et al., 1997; Fedje, 2006; Ford & Williams, 2007). Later flooding events may also erode and redeposit cave sediments. Glacial erosion may also have eroded former epikarst zones.

The cave system Svarthammarhola (SHC)

Scientific exploration of caves in Norway has taken place since the 1800s, and more systematically since the 1960s (Lauritzen, 2010). Most Scandinavian karst caves are of a minor volume (Lauritzen, 2010), with cave room dimensions of typically 1–2 metres modal width. The caves are usually described and quantified in terms of height, length and width upon surveying. More than 40 caves in Norway have dimensions of more than 1 km in cave passage length (www.speleo.no/dannelse/index.htm accessed 01.11.2018; Lauritzen et al., 2005; Skoglund & Lauritzen, 2010). The SHC system (Lauritzen et al., 2005) is situated at the northern part of the Mefjell massif, beneath a plateau next to the fjord valley Øvrevatn and SSE of the town of Fauske (Fig. 1A). The main passage chamber (Figs. 3 & 4) covers an area of approximately 40,000 m², reaching more than 100 m in width and several hundred metres in length, and is connected with smaller cave passages (Lauritzen & Mihevc, 2015). This passage chamber encompasses the largest volume of a cave room measured in Norway. The cave was discovered in 1969 by local cavers and published in a newspaper article (Andreassen, 1969), and the first map was produced in the following year (Heap, 1970). The SHC was resurveyed in several field campaigns throughout 2005–07 (Lauritzen, 2010), and work is still ongoing. Using compass, clinometer and laser distance-meter, aiming for ± 1 cm and ± 1° precision, vectors were measured from stations to stations, established throughout the cave passages, and on the land surface to connect to other smaller caves in the area. From selected stations within the main cave passages, more detailed vertical profiles of the roof and wall were created by measuring distance to the cave perimeter every 0.5–1°. This procedure may lead to uncertainties in positioning the cave in the rock mass beneath the plateau. Measurements were treated as polygon lines and imported into vector software Grottolf for cave visualisation (Lauritzen, 2008), and a coarse wall map for the main passages of the SHC is presented in Figs. 3 & 4. We used these data to construct top and bottom surfaces of the SHC, simplified for gravity modelling purposes.

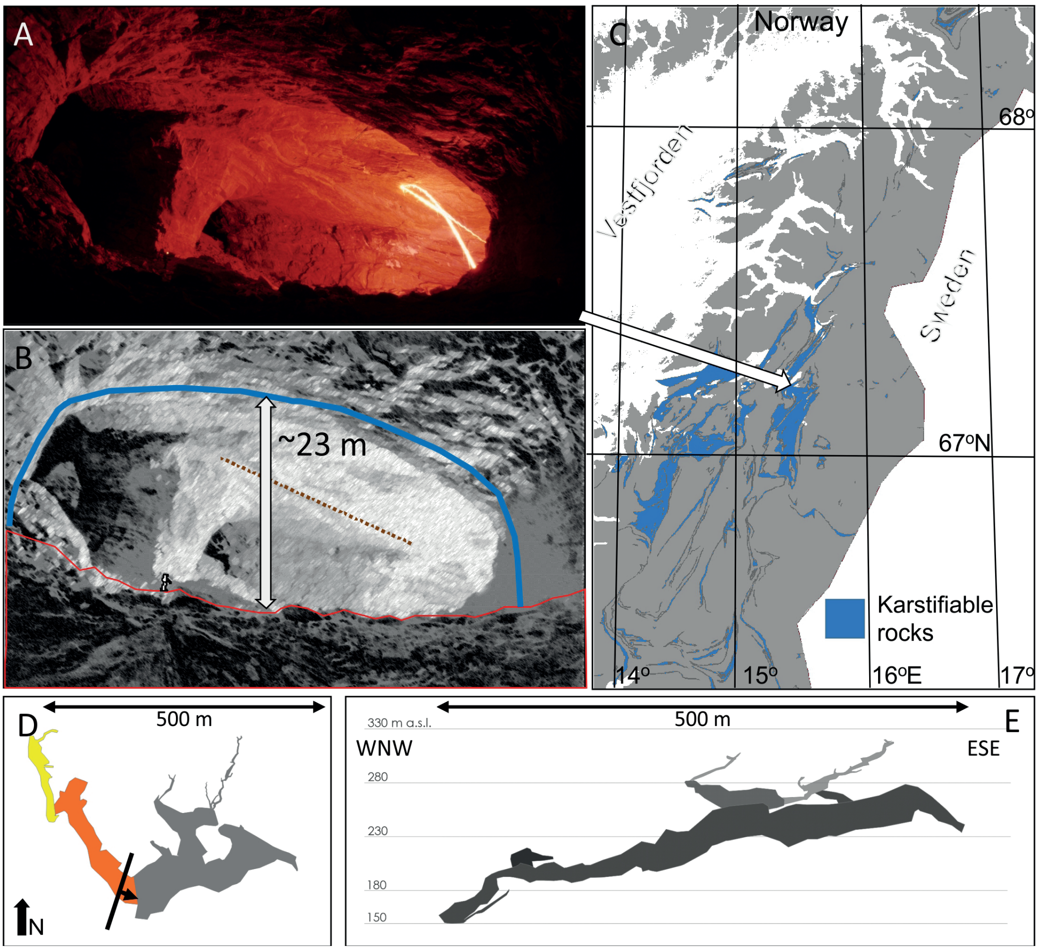

Figure 3. (A) shows a profile along a typical cave passage in the SHC and associated collapse sediment floor; for location of profile, see (D). (B) shows an outline of the same cave passage, with blue line marking cave passage roof and wall, and red polygon indicating sediments, stippled line marks foliation trend. (C) Map with major units of karstifiable rocks shown in blue colour (www.ngu.no/ and www.geonorge.no, accessed 01.12.2017). (D) shows horizontal outline of cave passages, lowermost part of cave (yellow), and area of ice mass occurrence (orange). (E) shows a stacked profile view with all SHC passages, the main passage in darkest grey. SHC drawn from data compiled and provided by S.-E. Lauritzen.

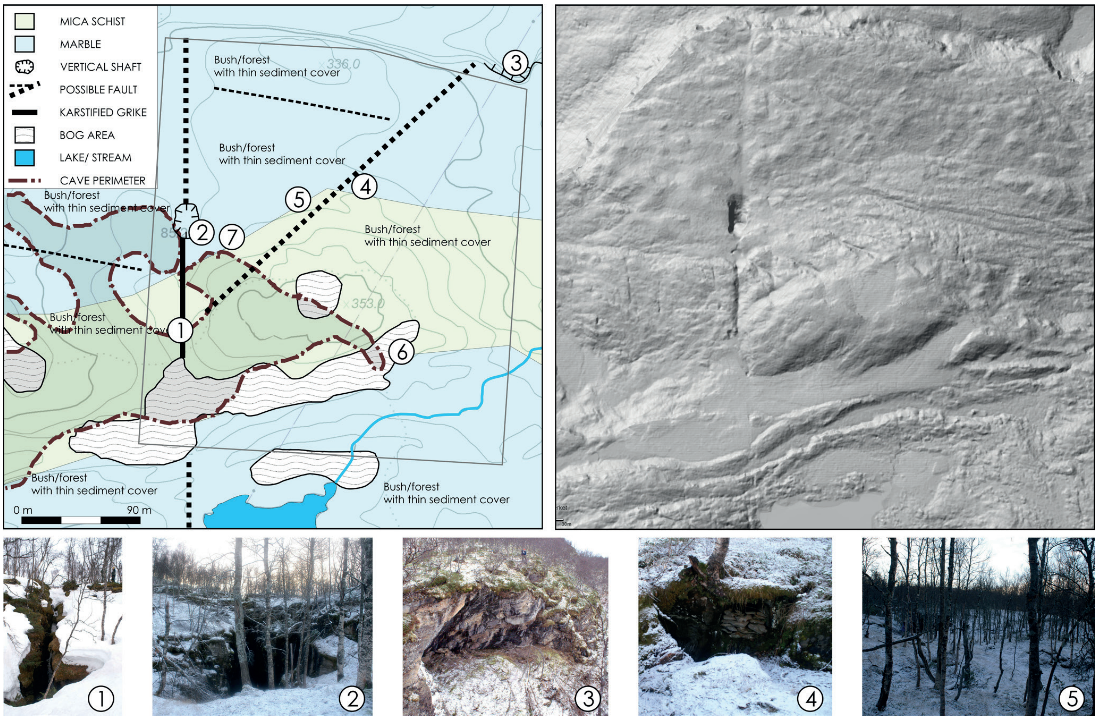

Figure 4 . Upper left: Topography map with areas that may contribute to density variations affecting gravity readings, see Fig. 1A for location, topographic contours (5 m spacing). North is up. Upper right: LIDAR-shaded relief map (2 points per m²), of same extension (www.hoydedata.no accessed 05.02.2018). 1 – shaft with small karst caves, 2 – collapse-filled karst pipe, 3 – rock shelter/possible cave entrance, 4 – smaller karst cave entrance, closed with old rock wall, 5 – general impression of area, 6 and 7 mark areas inside cave with indications of possible sediment-filled passages. Oblique rectangle shows data coverage area (Figs. 7, 10 & 11).

Dividing the major cave passages into cave room segments, the biggest single cave segment area measures approximately 90 x 140 m, and has a height of maximum 40 m. The vertical distance to the surface from the cave ceiling is 50 m or more, see Fig. 3E. From cave surveying, smaller cave passages (up to 1–3 m wide and 2–4 m high) continue under the northwestern part of the area of interest, in addition to the main room. Therefore, smaller and hidden cave passages are expected to be found close to the surface, especially in the northern part of the area of interest (Fig. 4).

The large passages in the SHC cave display significant collapse leading to modification of the roof and walls, with an elliptical dome-like passage profile appearance (Fig. 3A, B). The cave floor is not exposed in the main cave passage parts, due to a sediment cover of unknown thickness. The sediments are from visual inspection composed of collapsed debris from roof and walls, with scattered sandy deposits of glacifluvial origin, together with dust assumed to be originating from weathering of the host rock and later distribution around the cave. The depth down to the original cave floor may therefore be tens of metres.

The cave's roof collapse moved the open cave room stratigraphically upward into the micaceous rock mass, which also contains carbonaceous zones. From the NE side of the largest cave passage segment, there are indications of a cave passage collapse with sediments clogging up the continuation of the cave passage (Fig. 4: feature 7). In the SE corner of the same NE cave passage segment, the roof comes down into a sand-filled sump, which also may point to a continuation of the cave (Fig. 4: feature 6).

The plateau within the survey area exhibits a 30 m height difference, with the highest point being a hill in its southern part (Fig. 4). An investigation of the plateau topography above the cave (Fig. 4) shows that there are no signs of cave passage collapse at present day. On the western side, a depression with steep sides is interpreted as a vertical cave segment filled with sediments and can thus be referred to as a collapse pipe or breccia pipe. Within the SHC, the lower end of this vertical pipe can be recognised. The vertical distance from the bottom of the depression at the land surface is calculated (using Grottolf) to be ~40 m from the surface to the pipe shaft within the cave (Fig. 4: feature 2). Farther to the NE, approximately 200 m away from the NE wall of the main cave passage, a rock-shelter is found with the back wall consisting of what appears to be vegetation-covered collapse sediments. This rock shelter's back wall may indicate a possible collapsed/infilled entrance to a hidden continuation of the SHC (Fig. 4: feature 3). An elongated N-S shaft in the southwestern corner of the station grid is also karst related, with smaller entrances to minor karst caves (Fig. 4: feature 1). Furthermore, small karst caves are found scattered on the plateau (Fig. 4: features 4 and 5). Karst features may also be overlain by bog areas that dominate in the southernmost part of the survey area. These extend to unknown depth, but are assumed to be no more than a few metres thick.

Data and Methods

Petrophysical data

Marble, quartzite, mica schist, amphibolite and hornblende schist are encountered in the Mefjell massif (Fig. 1B). We used density values from several outcrops within a ten km radius from NGU's petrophysical database (Olesen et al., 2010). Minimum, mean, median and maximum density values were calculated, and are shown in Fig. 5 and listed in Table 1. We observe varying densities within the same rock type, explained by heterogeneous lithologies and metamorphic changes. The density values are in agreement with published ranges of 2400 to 2800 kg/m^3 for marble, and 2550 to 3100 kg/m^3 for schists in general (Dentith & Mudge, 2014).

Marble: For marble (n = 7), a wide range of 2610–2839 kg/m^3 is observed. Due to the affinity for karst dissolution, even lower density values are expected to occur. Also, inclusions are reported in marble some kilometres to the west (Roberts et al., 2001).

Schist: For the hornblende schist (sometimes conglomeratic) the densities vary from 2753 to 3031 kg/m^3, but the dataset is small (n = 4). The mica schist is described as rusty, with porphyroblasts of biotite and locally hornblende. Here, 24 measurements were available, with a large range, between 2663 to 2938 kg/m^3. The higher values may be due to porphyroblasts of heavier mineral assemblages.

Other rock types: Quartzite and amphibolite, though observed in the surroundings, are regarded as of minor occurrence and therefore not included in the modelling. Approximately 20 km farther west, pyroxenite is found within the same nappe.

Based on these measured densities from the surrounding outcrops, it is challenging to establish a precise background density value for the gravity modelling. Therefore, a likely scenario value with a density of 2770 kg/m^3 (Fig. 5) has been used, which would represent a rock composition of 75% marble and 25% mica/hornblende schist, reflecting the mean density values given in Table 1. The density of overlying bog accumulations, mainly water-wet organic material, is set to 1000 kg/m^3. Cave infill is here regarded as a mixture of non-consolidated glacifluvial and rockfall sediments with high porosities and is set to 1500 kg/m^3.

We present simplified scenarios in terms of possible karst features and host rock in Fig. 6, matured in the modelling process.

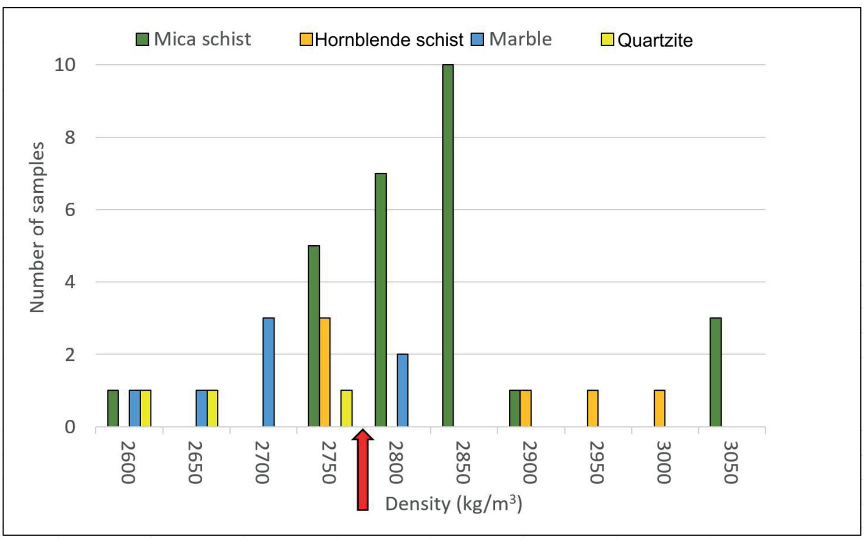

Figure 5. Distribution of density values. A density of 2770 kg/m^3 was chosen from a most likely scenario.

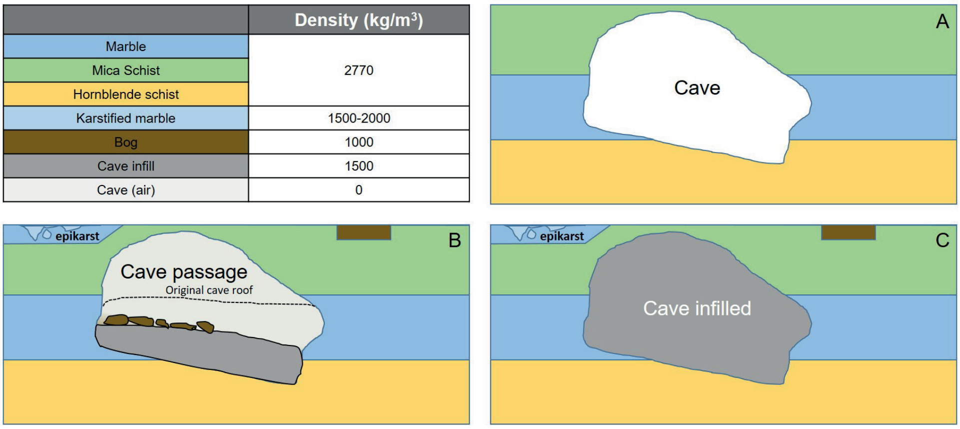

Figure 6. Concepts of karst cave in heterogeneous rock mass with (A) no infill, (B) low infill or (C) fully infilled, with rock types and densities used in the modelling.

Table 1. Statistical distribution of densities within a radius of 10 km from the cave area (https://www.ngu.no/emne/kartinnsyn, accessed 01.02.2018). Values are given as kg/m³ and n is the number of samples.

	Mean	*Minimum*	*Maximum*	*Median*	*n*
Mica schist	2836	2663	2938	2843	24
Hornblende schist and amphibolite	2936	2753	3031	2861	5
Marble	2731	2610	2839	2719	7
Quartzite	2693	2648	2774	2656	3
Pyroxenite	3139	3037	3280	3143	7

Microgravity data

A fieldwork campaign with gravity measurements was conducted during the late autumn of 2007 at the Mefjell massif on the northeast side of the plateau above the SHC, covering an area of approximately 280 x 300 m (Figs. 4 & 7). The station grid was designed to cover parts of the biggest cave chamber of the SHC, and an area where cave surveying and visual inspection on the land surface revealed the possibility of a cave continuation in an easterly direction.

Each gravity measurement was positioned with a Topcon differential L1-L2 GPS-GLONASS system. 95% of the gravity stations had dGPS positions determined to better than 10 mm horizontal and 20 mm vertical. Of the remaining stations, only 4 had vertical uncertainties exceeding 200 mm, with the worst being 511 mm. The setup was done with a reference station with a PG–A1 antenna and a kinematic rover connected to create a local digital elevation grid model with an approximate (20 x 20 m) cell size. Spike points were also established, and the cave was connected to the DGPS grid by continuing the cave survey on the outside to established DGPS points. The coordinate system used was WGS1984 UTM 33N.

Gravity data were acquired using a LaCoste&Romberg Model D gravimeter. In order to measure the drift, each station was visited two to three times, including a base station that was visited at the beginning and end of the survey day, and several times during each day. The drift was corrected with linear trends. Free-air corrections were applied to the gravity measurement period. Ocean tides were relatively small with a maximum seawater elevation change of 1.5 m (www.kartverket.no/sehavniva/tidevann-og-vannstand accessed 03.01.2017). The ocean tide gravity effect is calculated to be less than 0.1 mGal by gravity forward modelling. The vertical displacement range by solid earth tides has been calculated using the program *solid* (Milbert, 2018). The vertical Earth tidal movements vary within the range of 0.07 m to -0.15 m during the period of measurement. The gravity effect of the full range is calculated by applying the free-air gravity correction: 0.22 m x 0.3086 mGal/m = 0.068 mGal. However, both Earth and ocean tidal effects will be largely corrected by the drift correction, and are therefore not included as additional corrections.

Error estimations related to the processing steps are listed *in Table 2. Altogether, we estimate an error of* ± 0.2 mGal. Given the small area of interest, we neglect the latitude correction that would be almost constant within

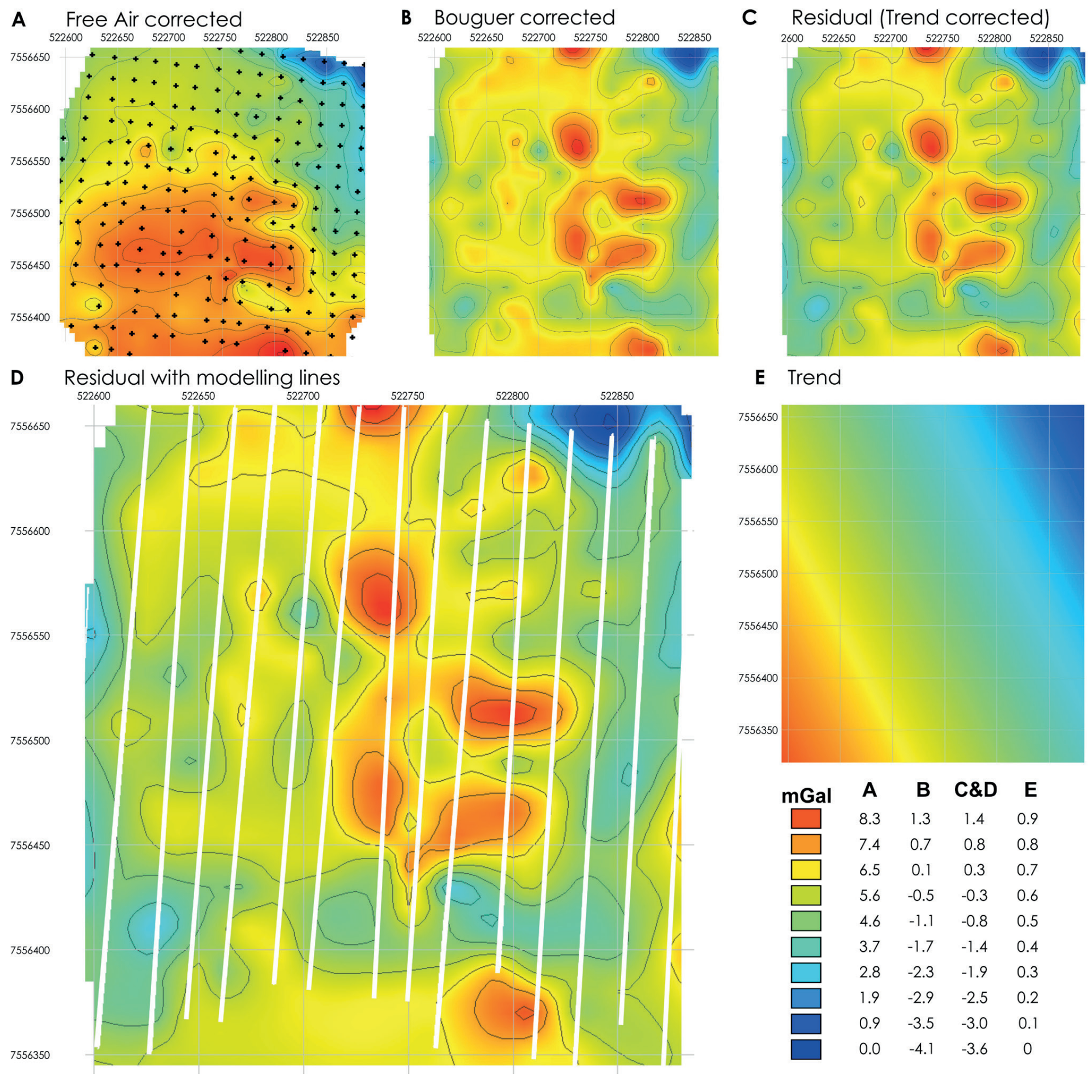

Figure 7. (A) Processed free air gravity grid and station locations (crosses), contour lines distance 0.5 mGal with gravity reading stations (black dots). (B) 3D Bouguer corrected grid. (C) Residual grid, trend corrected. (D) Trend corrected with modelling lines (white), oriented approximately N-S. (E) Regional trend.

the area. All measurements are kept as relative gravity values and have not been corrected to absolute gravity values. Our approach is common for microgravimetry (Ardestani, 2008; Beres et al., 2001).

The corrected gravity values were gridded with a grid cell size of 5 x 5 m and are displayed in Fig. 7, with Free air, Bouguer and residual anomalies. The same grid setup is used for the gridding of the DGPS data to make the digital elevation model.

Modelling and model parameters

Forward modelling and terrain correction were performed with software Modelvision (version 15, Tensor Research). A terrain model of the northern part of the Mefjellet mountain was constructed by converting the terrain into a body faceting the terrain surface. Facets are regular grid cells that increase in size from the centre towards the border of the area. The extent of this terrain model measures a total of 5.9 km in E-W

Table 2. Possible error sources from acquisition and processing.

Source error	*Explanation*	*Effect mGal*	*Correction strategy*
Gravity readings	Reading error, instrument handling incorrect.	unknown	Repeated readings.
Drift correction	Minor drift as proven by repeated base measurements.	Up to several mGal.	Applied to all points, no major drift during measurement period.
Free air correction	With dGPS height, generally sigma Z under 20 mm.	~0.01 mGal	Applied.
Terrain correction [3D Bouguer]	20 * 20 m grid, does not acknowledge smaller terrain differences.	Up to several mGal.	Applied, details in text.
Ocean tide correction	Modelled, less than 1.5 m tidal difference.	<0.1 mGal	Very small, not applied.
Earth tide correction	Modelled, see text.	~0,05 mGal	Very small, not applied.
dGPS measurements	XY: 95% of stations better than 10 mm horizontal	-	Extremely small, not applied.
Known cave position in rock mass	± 1° on compass and clinometer readings. Length by laser distance meter.	See Fig.1.	See discussion in text.

direction and 5.6 km in N-S direction. We used the DGPS measurements in the survey area, and a 10 x 10 m digital elevation model (DEM) outside the study area (www.geonorge.no accessed 01.12.2017). The latter is having a vertical uncertainty of up to 2 m. This terrain correction is a kind of a 3D Bouguer correction and was performed with the background density of 2770 kg/m^3 as derived from the density analysis described above. This background is used for all further modelling.

The next step was to construct a regional trend anomaly, which accounts for deeper sources in the Caledonian nappe structure. A regional gravity compilation (Fig. 8; 1 x 1 km grid cell size) was inspected for our wider study area. Inspection of this map shows a negative trend dipping towards the NE with an approximate 1 mGal/km within our grid area. Due to the low resolution of the regional grid, this trend can only give information on the variability of the trend on a large scale. However, minor variations on the scale of the study area are possible and cannot be derived from this data. Therefore, we derive the regional trend directly from the gravity data of the study area. Regional trends are commonly defined by polynomial surfaces (cf., Martínez-Moreno et al., 2015). We chose a tilted flat surface (polynomial degree 1) with the function R = a + bX + cY in order to preserve all shorter wavelengths in the study area. The parameters result in 'a' = 5832, 'b' = -0.00164798 and 'c' = -0.00083891. The critical parameter is the offset 'a'; too small offsets will result in too high densities and vice versa. Modelling

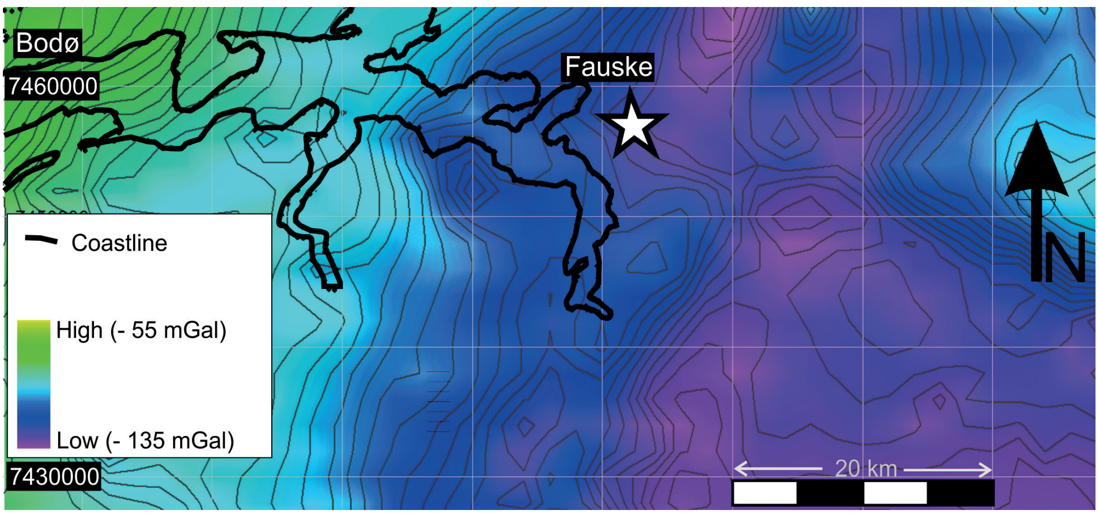

Figure 8. Bouguer gravity map of the Salten area, 1 x 1 km grid cell size (Geological Survey of Norway: Gellein, 2003; Olesen et al., 2010). Note NNE–SSW-trending gravity trough with an apparent offset towards east at SHC position (star), a possible indication of regional WNW–ESE-trending fault system.

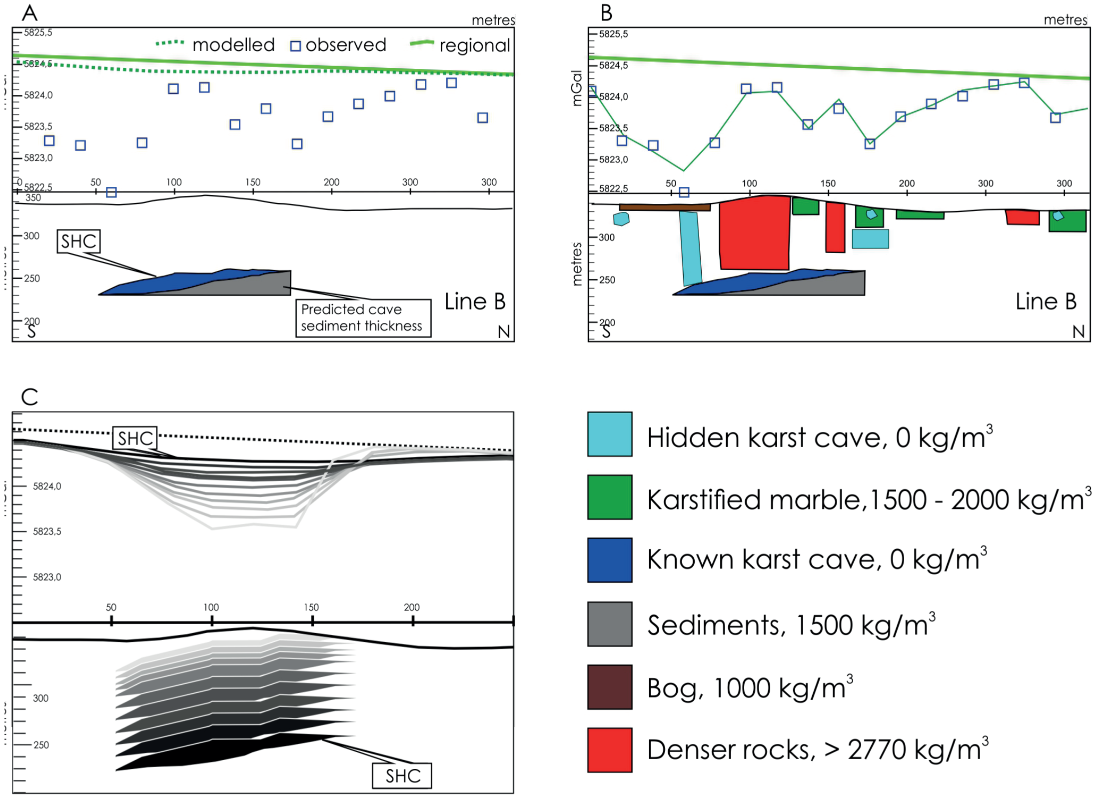

Figure 9. *(A) shows line B (see Fig. 12 for location) modelled with known SHC geometry and estimated sediment thickness effect at cave floor, resulting in a small anomaly. (B) shows the same line, now fully modelled to explain the observed signal. (C) Gravity anomalies of cave Svarthammarhola (SHC), modelled at known position (black) shown together with gradual uplift towards the plateau with modelling result in corresponding grey scale. For location see Fig. 13, line B.*

tests varying the offset were performed and we found that the offset 'a' = 5832 mGal resulted in the most reasonable densities. The small size of the parameters 'b' and 'c' indicates a very small tilt. The regional trend used in the modelling is shown in Fig. 7.

Modelvision software builds the geometry of the subsurface by inserting bodies of different shapes into the subsurface volume. The bodies' densities as well as the background density for the subsurface volume needs to be set by the user. All bodies within the subsurface volume contribute to the gravity anomalies. This framework defines a 3D environment with 3D bodies. Body geometries can be modified in vertical profiles or in the map plane. We use the following body types:

- Horizontal prisms, defined by its polygonal cross section in profile and/or map view, where strike angle, strike lengths and plunge can be modified.

- Frustums, with their top and bottom defined by topographic surfaces in the map plane.

The SHC cave ceiling and cave floor were exported from the Grottolf Software, imported into the Petrel software (Schlumberger) and exported to Modelvision as grid surfaces, in order to create the SHC body. An intermediate wavelength anomaly is produced by the known cave, with an anomaly strength of approximately 0.3–0.4 mGal, see Fig. 9. This calculated gravity anomaly is compared with the measured anomalies, shown in Fig. 10. The observed anomalies are smaller in wavelength and larger in anomaly size, which clearly indicates that additional shallow sources are needed (Fig. 10C).

Subsequently, further bodies were created with densities which differ from the background density in order to achieve a match between modelled and measured gravity anomalies, as well as to honour the observed geological features in a geologically realistic way (Fig. 11).

Our workflow for the data collection, processing and modelling is summarised in Fig. 12, and advantages and suggestions for improvement will be discussed below.

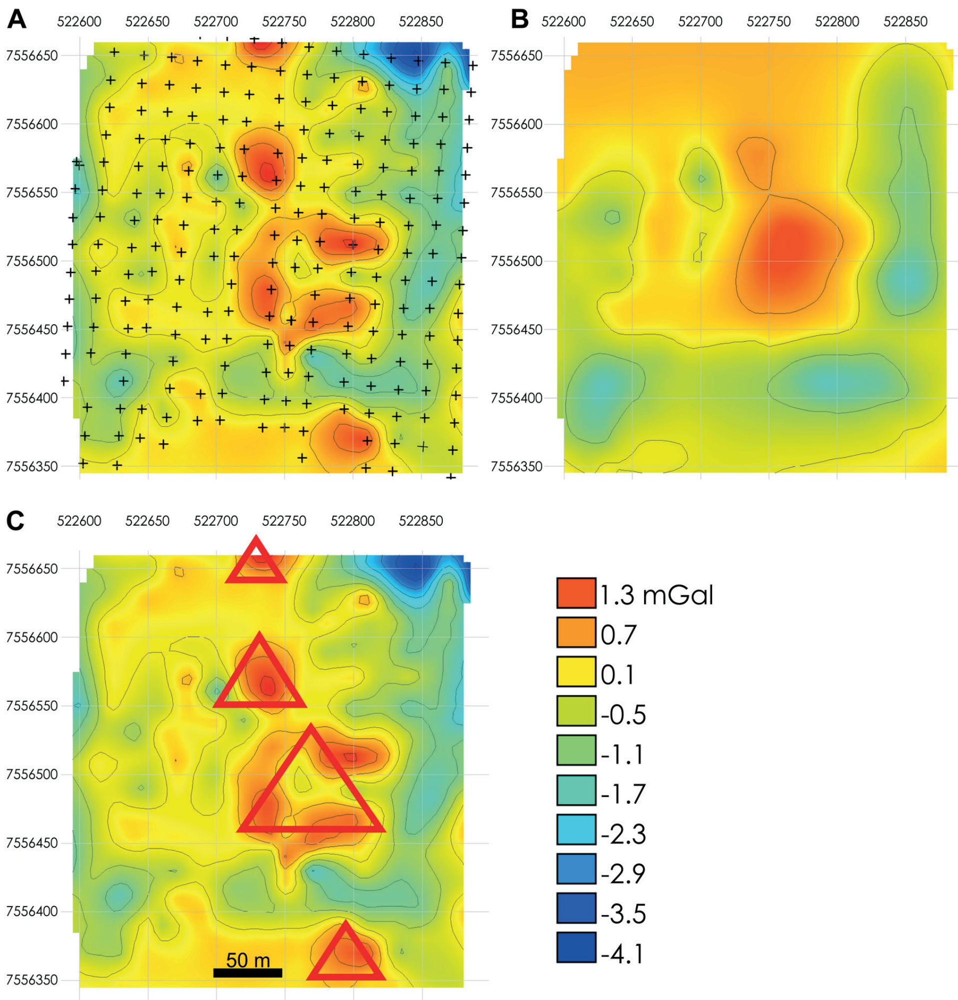

Figure 10. (A) The Bouguer corrected grid with gravity reading stations. (B) Calculated anomalies from model (residual). (C) Areas marked with red triangles indicate areas with very high densities.

Modelling results

The most plausible model result is shown as maps, sections and 3D displays in Figs. 11, 13–16. Fig. 9B shows an example for a modelling profile passing both the SHC and major and minor hidden caves and karstified bedrock. The shaft at the left side of the SHC in Fig. 9B coincides with the largest negative anomaly, but no indications for this feature are found at the surface. This anomaly is defined by several points, therefore we regard the signal as trustworthy. From Fig. 11B, D, two main trends of karst occurrences can be recognised: a karstified zone above the SHC, extending towards north, and a possible prolongation of the SHC towards east, which bends after ~150 metres towards north.

Fig. 13 shows the sections with the hidden cave passages, karstified marbles, known karst caves, collapse breccia pipes, sediments and bog. Fig. 14 shows a 3D view of the entire SHC and the modelled hidden cave passages, with their altitudes highlighted by different colours.

The calculated gravity anomalies of this model are shown in Fig. 10 in comparison with the observed anomalies and show a good match for the longer wavelengths. The positive anomaly, marked by the largest red triangle in Fig. 10C (section F to J in Fig. 13), cannot be modelled within our density range for the rocks found in the area, and requires introducing higher densities as discussed below.

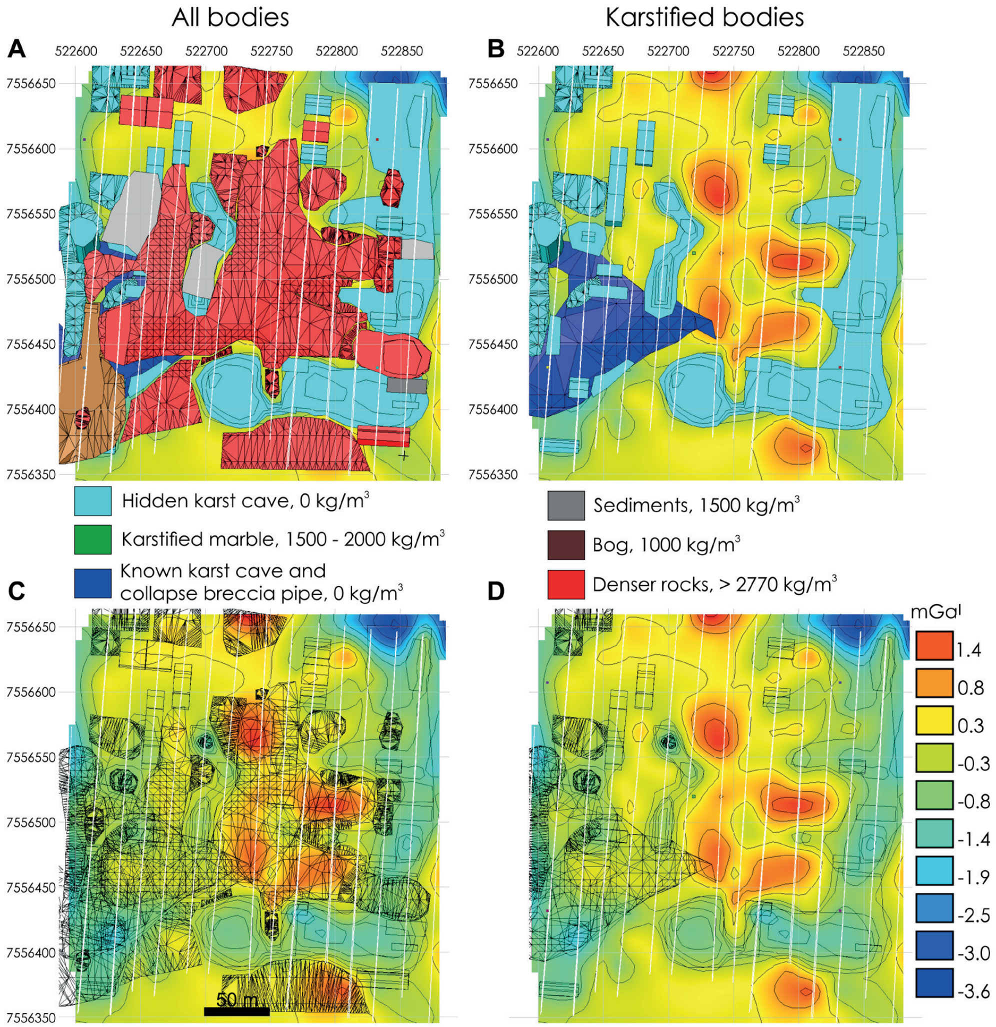

__Figure 11.__ Overview of bodies with overlain Bouguer corrected grid, with (A) and (C) showing all bodies both filled and as wire-frame bodies. (B) and (D) show only karstified bodies filled and as wire-frame bodies.

Modelled scenario uncertainties

Due to inherent non-uniqueness of the gravimetry method, theoretically an infinite number of models could explain the observed gravity signals. However, by using geological knowledge and reasonable density values we can effectively constrain the models. We here present three different approaches for introducing uncertainties into the model, and argue for our choice of the most probable scenario that can be achieved with this type of data.

Geometry: The geometrical shapes of the deep hidden caves are strongly simplified, and are shown as boxes, as the anomalies from this depth cannot resolve complicated shapes. Uncertainty also relates to the precise depth of the cave. Moving the cave down into the rock mass, implies increasingly larger cave bodies to explain the same observed signal (Fig. 9C). We therefore investigated a 'larger cave' model scenario (Fig. 15). Although both models shown in Fig. 15 match the observed gravity signal, the 'larger cave' scenario (Fig. 15B) would most likely experience roof collapse, which would be visible from the surface, and no signs of such collapse features are seen at the plateau.

Our interpreted structures at shallow depth coincide with realistic cave passage dimensions, regarding cave stability (Lauritzen & Mihevc, 2015).

The hidden cave passage height in this southern part is

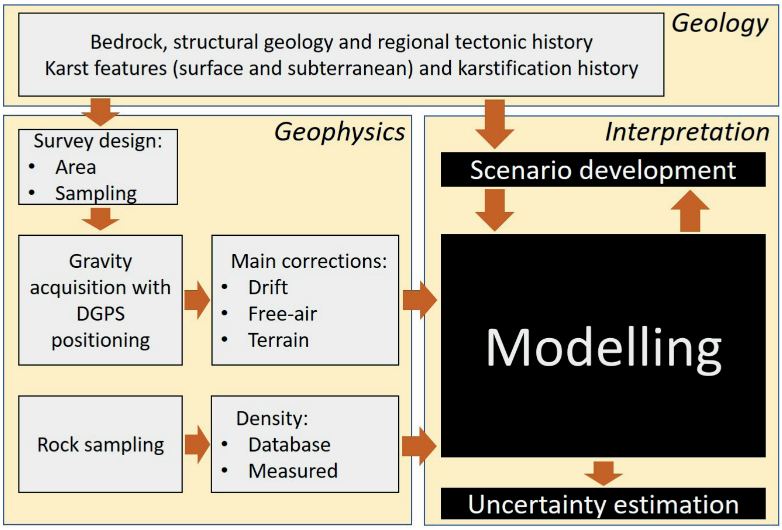

Figure 12. Proposed workflow for gravity exploration of cave passages.

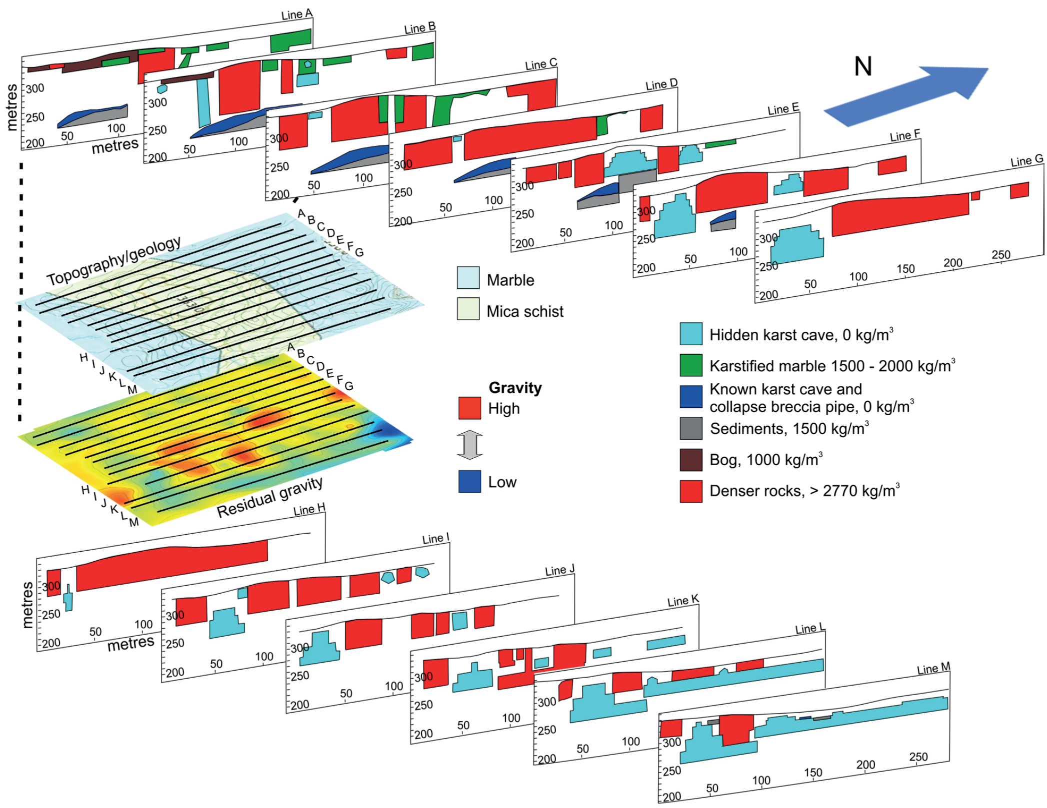

Figure 13. 3D presentation of all modelled sections, their position stated on the topography/geology map and residual gravity map. See also Figs. 11 & 14.

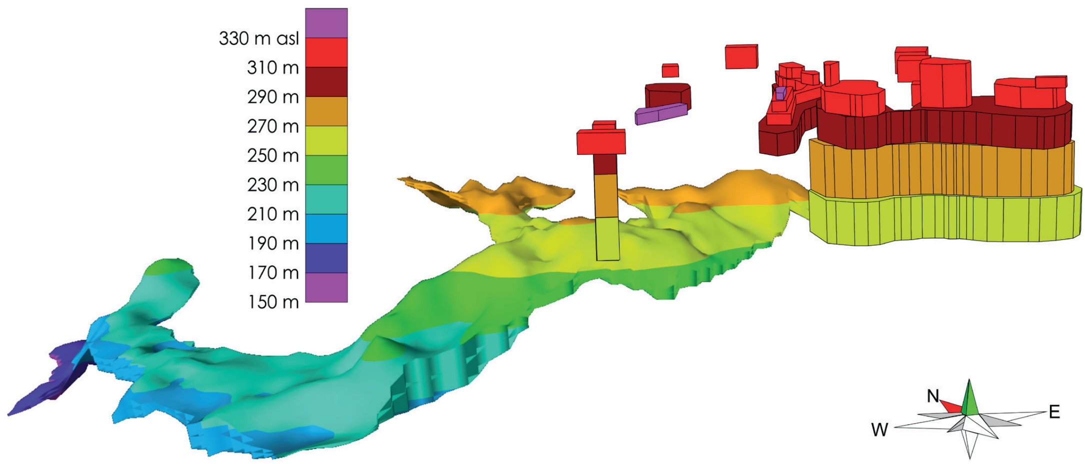

Figure 14. 3D model showing the known SHC to the left (smoothed horizons) and modelled hidden caves to the right (blocks), seen from SSW. Note large vertical height of the hidden caves.

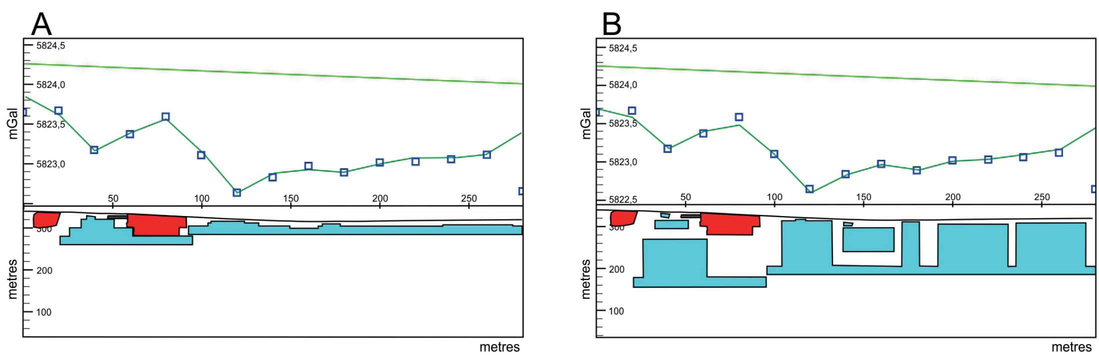

Figure 15. Modelling with two different cave ceiling depths on line M, see Fig. 13 for the position. (A) The modelled cave room with best-fit. (B) Base of cave positioned 100 m downwards into the rock mass.

twice the size of the SHC passage maxima. This may be explained by the cave passage being partly controlled by a steeply dipping, E-W-striking fault. The existence of this fault trend gains support from the lineament observations at the surface (Fig. 4), as well as the regional fault trend on the regional gravity map (Fig. 8). However, only a detailed in situ cave survey of the hidden cave will reveal the exact geometry of the hidden cave passages.

Cave infill: Uncertainties relate to different scenarios of the cave interior, the simplest being air-filled cave passages with a density of zero. Sediment-infilled cave passages lead to a lower gravity anomaly of the cave body. This must be compensated by a larger cave room to match the gravity response. Different sedimentological processes may give a different fabric laterally and vertically, and consequently a varying average density of the unconsolidated sediments. It is possible to encounter collapse breccia from cave roof and wall collapse, in addition to diamictons, fluvial and lacustrine sediments mainly of a glacial origin, water bodies and ice. All of these sediments are observed within the SHC today and/or on the plateau and surroundings. We therefore expect a density range of 1300–1700 kg/m^3; and as we do not know the composition of possible sediments in the hidden cave rooms we used an average of 1500 kg/m^3.

Water-filled cave passages are not observed in the upper part of the known cave, but are found in the lowermost western part outside our area of interest, near 150 m a.s.l.. Therefore, we do not expect standing water bodies to be encountered in the hidden cave passages, which are positioned close to the hinge line of a NNE–SSW-trending antiform (Fig. 16).

Within the SHC, a large ice body is situated in the western lower part of the cave, outside our study area. The cave ice is situated below the lowest cave entrance. The ice is regarded as stagnant today but shows signs of former movement, indicating that it used to be part of an active glacier. The special micrometeorological conditions within the SHC create a ventilation 'chimney effect' that freezes, preserves and cools the cave ice mass during the wintertime (Baastad, 2006). At present conditions there is a negative accumulation trend and loss of ice mass due to ablation. Therefore, we do not expect ice in the hidden cave rooms.

Host rock: A further uncertainty is linked to the choice of background density. A higher background density will lead to smaller cave rooms, but the characteristics of the geometry will be preserved. We have already discussed in the introduction that karstification does not provide just the (larger) cave void in the host rock, but also affects the host rock by creating the epikarst zone, which comprises a wider pore/permeability system than what can be seen from entering a cave (Fig. 6B, C). Furthermore, unconsolidated sediments, either by collapse or other sedimentary processes (glacial and/or glacifluvial deposition, weathering, etc.), may also reduce this epikarst density contrast. Adding 'denser' autochthonous sediments of possible siliciclastic origin may mask the epikarst porosity, together with fluids (e.g., groundwater table) filling the remaining pore space. This could both lower and increase the overall density contrast within the carbonate host rock.

Small caves may not be visible from outcrops, as they are often buried under sediment cover, but may still be

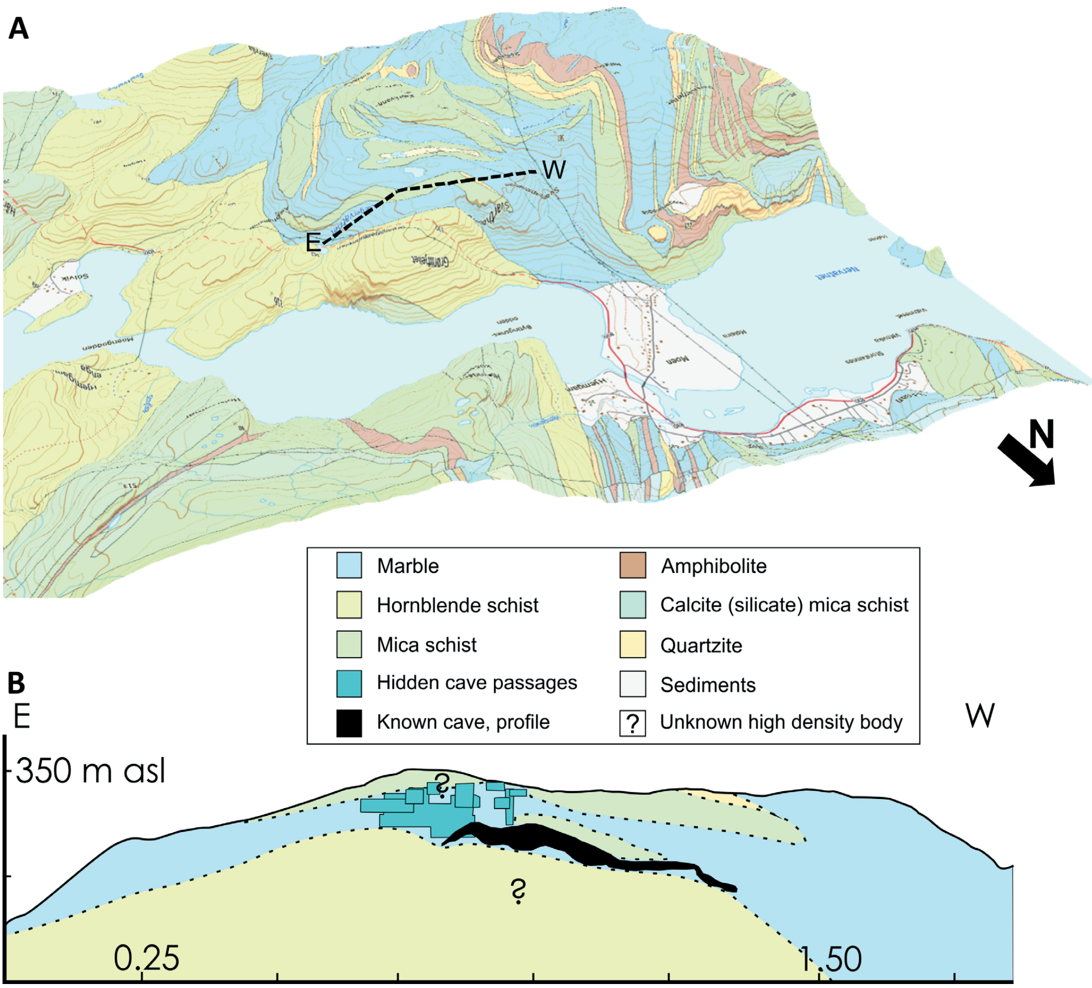

Figure 16. (A) 3D view of the Mefjell antiform, geological map (Fig. 1B) with profile indicated for (B). (B) Vertical profile through the Mefjell antiform of the simplified cave passage of SHC, and position of modelled hidden cave passages. Lithological boundaries are extrapolated from the geological map and cave inspection; for exact profile position see Fig. 1B.

plentiful within the rock mass. Their presence will lower the overall density of the rock.

The heterogeneous nature of the composition of the rocks in the Mefjell area, together with their folded appearance gives an additional challenge. The different observed densities in the mica schist can be attributed to impurities by both the presence of local carbonates within the mica schist (karstifiable and therefore reducing the overall density), as well as the presence of denser mineral aggregates or by local denser rock bodies of pyroxenite or amphibolites increasing the density. Furthermore, the geological map (Fig. 1B) in this folded terrane may not reveal all the rock types in the subsurface in our area of interest.

Most probable scenario: The results indicate that a larger part of the overall cave rooms must be present as an empty (non-filled) room that should be accessible by digging or drilling, as the gravity anomaly cannot be modelled using sediment infill in the hidden cave passages. Therefore, open hidden caves are most likely to be encountered.

Discussion

Workflow

Based on our modelling approach in full 3D, we here present an improved workflow (Fig. 12) for using the gravity method to detect karst in a Caledonian nappe setting. Using known geology (bedrock, structural geology and regional tectonic history) combined with local observations of karst features and ongoing interpretation of karstification history is the preferred starting point. This is the basic input for the survey design and processing including necessary corrections, together with rock density properties either from our own samples or local/regional databases. This also provides the foundation for scenario development before modelling and uncertainty estimation.

It is important for future application of the gravity method in complex structural settings to gain a rough understanding of where one can expect possible karstified rooms, at what depth and lateral extent. It is also beneficial to expand the area of interest into the non-karstified area. It is suggested to gather a few longer (regional) profiles in addition to the study grid in order to capture larger wavelengths related to deeper structures, and to gain a better understanding of the background trend of the gravity anomalies. Detailed geological mapping with rock sampling is another benefit.

This method can also be applied in other settings where gravimetry is considered an option. In a wider view, gravity exploration can be integrated with other geophysical methods that can be used to address the search for hidden cave passages, such as ground penetrating radar (e.g., McMechan et al., 2002), electrical resistivity imaging or electrical potential differences (e.g., Kaufmann et al., 2015).

Continuation of the SHC and geological context

The overall geology beneath the plateau comprises an antiform with three main lithological units (Figs. 1 & 15). This is a simplified view and does not incorporate the heterolithic composition within the different units, nor does it acknowledge undulating lithological boundaries. While this adds uncertainties to the geometries of our model, it can be stated without doubt that open cave rooms of appreciable size exist, along with trends that can be trusted.

The modelled result also gains support from regional lineament trends (Fig. 1A). The main NE-SW foliation trend coincides with the orientation of the largest cave chamber in the SHC (outline in Fig. 4). The E-W trend of the southern part of the hidden cave matches with another known SHC trend, and is also recognised from regional lineament trends (Fig. 8). The N-S trend of the eastern part of the hidden cave is recognised in the N-S-trending lineament in the western part of the grid (Fig. 4) which we interpret as a possible fault zone as discussed above. Fault zones are prone to karstification due to weakening of the host rock. A N-S trend is also recognised in the regional Bouguer gravity map (Fig. 8) which places the Mefjell massif into the southern part of a much larger N-S-trending gravity trough. Finally, we observe that the newly interpreted hidden caves together with the known SHC system are positioned at the top of the hinge line of a large antiform (Fig. 16).

Our model expands the present-day known SHC system (Lauritzen et al., 2005) in an eastward and northward direction. The modelled hidden caves consist of air-filled passages, matching with both suspected SHC continuations and an outside rock shelter. This is a strong indication that the modelled hidden cave systems and the SHC were previously connected. This connection is today choked by sediment infill. The largest modelled hidden caves have a similar volume and geometry as the SHC (Figs. 3 & 15).

Speleogenesis

The characteristics of the extended SHC cave system are intriguing and are here discussed in the light of speleogenesis (initiation of the cave). In the following, we review the speleogenesis of the SHC and surrounding caves, and discuss arguments for a possible hypogene origin. The speleogenesis and evolutionary history of the SHC are uncertain; one speleothem from the SHC is dated, a stalagmite/flowstone plate, giving Eemian and Early Weichselian ages (Fedje, 2006). However, the speleothem was not found in situ, but is believed to have been redeposited close to its growth position within the SHC. This date therefore provides a minimum age for the SHC given that the flowstone was originally precipitated in the cave. In Lauritzen (1990), ages for the speleogenesis of the SHC are discussed and the author concluded with the uncertain possibility of a pre-Quaternary age due to the cave's position under a possible paleic surface.

The SHC including hidden passages comprises a cave system of extraordinary size. Other cave systems with an overall similar size to the SHC have not been reported from the Nordic countries, even though some caves exhibit minor passage elements measuring similar dimensions. The SHC has previously been suggested by Lauritzen (1990) as the erosional remains of a larger cave system. Other prominent caves in the immediate neighbourhood are the Solvikhola arch and the Okshola–Kristihola cave system.

Solvikhola arch: A few km east of the SHC along the fjord valley, approximately two hundred metres altitude lower, this cave arch (Fig. 1A for location) displays a similar cave passage diameter. It has been suggested to be an erosional remnant of a larger paleo-cave system (Lauritzen, 1990).

Okshola–Kristihola cave system: North of the Mefjell massif, across the fjord valley, speleothems in this cave system (Fig. 1A) have been dated, providing ages corresponding to earlier interglacials than Eemian (Skoglund & Lauritzen, 2010). The cave system displays a major vadose incision in its lower parts, where a more than 50 m-high passage relief developed due to gravitational-controlled fluvial incision (Skoglund & Lauritzen, 2010).

Combining the SHC's position at the top of the hinge of a large antiform, where we also modelled uncommonly high densities, together with the cave's outstanding size, opens for a new interpretation of the speleogenesis. The hinge of an antiform is commonly a focal point for fluids migrating from greater depths. Therefore, could the SHC system be related to hypogene (hydrothermal) karst, with a possible downward continuation of the cave passages into greater crustal depths (Klimchouk, 2014)? A hypogene origin would require upwelling groundwater circulation from the lithosphere with hydrothermal fluids and/or sulphuric gases. The antiformal setting dipping southwards into the rock mass could provide a route for deep-seated fluids migrating towards the SHC. As earlier discussed, high-density bodies are required due to the constraints of the known structure and lithology (Figs. 10C & 11A), which could also be explained by a paleokarst setting with cave passages infilled by ore deposits, or the cave room is infilled with lithified sediments or diverse precipitates. Another possible explanation could be that within the carbonates we may find Mississippian Valley Type ore deposits, as known from United Kingdom, USA and elsewhere (Leach et al., 2010).

In a hydrothermal system one may also expect deposition of gypsum/anhydrite in substantial amounts, but these are not known from the SHC. However, the preservation of evaporites is doubtful as late glacial flushing episodes of melting water would probably dissolve or erode such deposits, with collapse material filling in any passage extension continuing deeper down into the crust.

A related question is where would other cave passages from the same deeper hypogene system reach the present-day surface? Solvikhola may be a candidate to be part of such an extensive system, whereas the larger cave passages of the Okshola–Kristihola cave system have been explained as a product of meteoric karst alone (Skoglund & Lauritzen, 2010).

With our present knowledge we cannot distinguish between a meteoric and a hypogean origin for the SHC. The hypogene hypothesis can only be tested by invasive sampling in the known and hidden cave system, combined with further geophysical exploration.

Offshore analogues

In hydrocarbon and groundwater exploration studies, karstified rocks are loosely described as rocks with secondary porosity on a wide range of scales. Such rocks can form important reservoir rocks for groundwater or hydrocarbons. Recent hydrocarbon discoveries in carbonate rocks from exploration wells in the Norwegian sector of the Barents Sea are the wells 7120/1–3 'Gohta', 7220/11–1 'Alta' and 7220/6–2 'Neiden' (www.npd.no accessed 03.01.2018). In those exploration settings, karstic properties may be challenging for drilling and production. Conductive pathways due to caves and other karst features potentially create zones of extreme permeability, which along with the occurrence of highly heterogeneous rock properties may affect the sealing and lead to the establishment of leakage routes through the reservoir overburden.

Our near-surface observations also have implications for detecting and interpreting large karstic cave systems in offshore settings at much deeper depths, an example being the karstified reservoir at 2 km depth below the sea surface in the 7220/11–1 'Alta' discovery offshore northern Norway. As discussed in the introduction (Fig. 2), gravity anomalies decay with increasing depths and also lose short-wavelength information. Therefore, gravimetry is not the preferred method for detecting large cave systems at such depths, but could potentially detect karstified rock volumes due to the established fact that the overall density of the host carbonate body is lowered. For the SHC case, the low density anomaly is not only attributed to larger caves but also the epikarst zone. This epikarst zone may be thicker than 10 m in a near-marine setting and also be laterally very extensive, as fluctuating sea levels over time would give further dissolution together with widening and expansion of cave systems (Mylroie & Mylroie, 2007). This modelling study may therefore provide a useful analogue for quantifying the expected gravity anomalies in deeper karst systems.

Environment

Caves, due to their low energy environment, can also be important sedimentary archives for the natural history of the surrounding area and for the geological history of the cave itself. They are thus vulnerable for destruction by human entry (Lauritzen, 1991; Ford & Williams, 2007). In our area, we have an incomplete sedimentary record since glacial erosion has removed and/or redistributed sediments and rocks on the surface (e.g., Andersen, 1975; Mangerud, 2004). The implications of this, if further investigations confirm our interpretation of a hidden cave, are important and not without complications. The possibility of encountering sediments and speleothems of a Neogene age or older, susceptible for dating, is intriguing and should be a focus for further work. The hidden continuation of the SHC may contain important and unknown clues, from sediment infill and other speleothems, for the natural history of the area. Due to the vulnerable underground environment and the value of potential natural history data; e.g., zoological, glacial, and vegetational history to be extracted from the cave, a careful and planned investigation must take place to make sure that all possible information is retrieved in a sound, scientific way.

Summary

1. We have demonstrated how gravity field – surveying and modelling – is a useful tool for the detection of hidden cave passages in complex orogenic nappe settings. The results of this shallow subsurface exploration of karst features in the gravity data give useful constraints for the potential use for gravity field data also in mapping more deeply buried karstified terrain.

2. We present a workflow for gravity investigation where there is potential for detection of hidden cave passages.

3. Observed gravity lows have been interpreted as hitherto unknown and inaccessible cave rooms, some of which correspond with collapse features seen in the Svarthammarhola (SHC), and from a rock shelter at the surface. This expands the known cave system in an eastward and northward direction.

4. Interpretation challenges are related to density variations caused by heterogeneous lithology of the host rock, zones of karstification (epikarst, smaller karst caves, etc.), and sediment infill leading to lower density contrasts. These challenges have been addressed by testing different density values for different scenarios, based on observations in the SHC.

5. Some gravity highs indicated the presence of high-density rocks, where amphibolites, pyroxenites or hydrothermally altered carbonates are regarded as quite probable.

6. Combining the cave's position at the top of the hinge of a large antiform, where we also modelled uncommonly high densities, together with the cave's outstanding size, opens for new interpretations of the speleogenesis. We infer a hypogene karst origin. This issue should be addressed in further work, including geochemical investigations and by applying other geophysical methods.

Acknowledgements. The present study was conceived by Stein-Erik Lauritzen, (SEL) under the Svarthammar Research Project (Norwegian Research Council, Norpast2; Lauritzen et al., 2005) and initial fieldwork funded through the Department of Earth Sciences, UiB ('såkornmidler') to him and Arne Gidskehaug. The task was later merged into a PhD project for Terje Solbakk (TS), supervised by SEL and Walter Wheeler (WW) at the University of Bergen and Center of Integrated Petroleum Research. WW and TS thank The Norwegian Research Council for field expenses and salary support (NFR 176132, Paleokarst Reservoirs: An integrated 3D approach to heterogeneity, reservoir- and seismic modelling). NGU is thanked for loan of DGPS equipment and kind permission to use gravity data. The presented study is finalised as a part of TS' PhD project under the ARCEx project (Research Centre for Arctic Petroleum Exploration) which is funded by the Research Council of Norway (grant number 228107) together with 10 academic and 9 industry partners. We thank Arne Gidskehaug, Kjetil Broberg, Bjørn Solbakk, Tor Inge Korneliussen, Sylvia (Vangen) Slåttkjær and Hans-Martin Slåttkjær for their assistance during the fieldwork, and Terje Larsen and his family for their hospitality. The authors also wish to thank Marco Brönner and Odleiv Olesen for helpful discussions. We want to express our sincere thanks to Zuzana Alasonati Tašárová and an anonymous reviewer for improving our manuscript.

References

Agyei-Dwarko, N.Y., Augland, L.E. & Andresen, A. 2012: The Heggmovatn supracrustals, North Norway—A late Mesoproterozoic to early Neoproterozoic (1050–930Ma) terrane of Laurentian origin in the Scandinavian Caledonides. *Precambrian Research 212*, 245–262. https://doi.org/10.1016/j.precamres.2012.06.008.

Andersen, B.G. 1975: *Glacial geology of northern Nordland, North Norway*. Universitetsforlaget, Trondheim, 74 pp.

Andreassen, K.A. 1969: Bergtatt. In newspaper: Nordlands Framtid, Bodø. Date 11.10.1969.

Ardestani, V.E. 2008: Modelling the karst zones in a dam site through micro-gravity data*. *Exploration Geophysics 39*, 204–209. https://doi.org/10.1071/EG08022.

Baastad, L. 2006: Ventilasjonseffekter og mikroklima i Svarthammarhola i Fauske. MSc thesis, University of Bergen, 82 pp.

Barrows, L. & Fett, J.D. 1985: A high- precision gravity survey in the Delaware Basin of southeastern New Mexico. *Geophysics 50*, 825–833. https://doi.org/10.1190/1.1441957.

Beres, M., Luetscher, M. & Olivier, R. 2001: Integration of ground-penetrating radar and microgravimetric methods to map shallow caves. *Journal of Applied Geophysics 46*, 249–262. https://doi.org/10.1016/S0926-9851(01)00042-8.

Braitenberg, C., Sampietro, D., Pivetta, T., Zuliani, D., Barbagallo, A., Fabris, P., Rossi, L., Fabbri, J. & Mansi, A.H. 2016: Gravity for Detecting Caves: Airborne and Terrestrial Simulations Based on a Comprehensive Karstic Cave Benchmark. *Pure and Applied Geophysics 173*, 1243–1264. https://doi.org/10.1007/s00024-015-1182-y.

Butler, D.K. 1984: Microgravimetric and gravity gradient techniques for detection of subsurface cavities. *Geophysics 49*, 1084–1096. https://doi.org/10.1190/1.1441723.

Chico, R.J. 1964: Detection of caves by gravimetry. *International Journal of Speleology 1*, 101–108. https://doi.org/10.5038/1827-806X.1.1.11.

Dentith, M. & Mudge, S.T. 2014: *Geophysics for the Mineral Exploration Geoscientist*. Cambridge University Press, 9780521809511. https://doi.org/10.1017/CBO9781139024358.

Drivenes, K., Sørensen, B.E. & Larsen, R.B. 2016: Orogenic degassing, scapolitization and K-metasomatism during Caledonian exhumation, Helgeland, Norway. *Norwegian Journal of Geology 96*, 223–244. https://doi.org/10.17850/njg96-3-04.

Fedje, E. 2006: A paleoclimate proxy record for the Fauske area based on the stable isotope record preserved in speleothem and dated by the TIMS method. MSc thesis, University of Bergen, 168 pp.

Ford, D. & Williams, P.D. 2007: *Karst hydrogeology and geomorphology*. John Wiley & Sons, 978-0-470-84996-5, 576 pp. https://doi.org/10.1002/9781118684986.

Gellein, J. 2003: Gravimetrisk residualkart, Sulitjelma, scale 1:250,000, *Norges geologiske undersøkelse*.

Heap, D. 1970: Report of the Speleological Expedition to Arctic Norway. William Hulme's Grammar School. 21 pp.

Kaufmann, G. & Romanov, D. 2009: Geophysical investigation of a sinkhole in the northern Harz foreland (North Germany). *Environmental Geology 58*, 401–405. https://doi.org/10.1007/s00254-008-1598-0.

Kaufmann, G., Nielbock, R. & Romanov, D. 2015: The Unicorn Cave, Southern Harz Mountains, Germany: From known passages to unknown extensions with the help of geophysical surveys. *Journal of Applied Geophysics 123*, 123–140. https://doi.org/10.1016/j.jappgeo.2015.10.004.

Klimchouk, A. 2014: The Methodological Strength of the Hydrogeological Approach to Distinguishing Hypogene Speleogenesis. *In* Klimchouk, A., Sasowsky, I.D., Mylroie, J., Engel, S.A. & Engel, A.S. (eds.): *Hypogene Cave Morphologies*, Selected papers and abstracts of the symposium held February 2 through 7, 2014, San Salvador Island, Bahamas, Karst Waters Institute Special Publication 18, Karst Waters Institute, Leesburg, Virginia, pp. 4–12. https://doi.org/10.13140/2.1.1187.3287.

Kollung, S. & Gustavson, M. 1995: Rognan. Berggrunnskart; Rognan; 21293, scale 1:50,000, *Norges geologiske undersøkelse*.

Lauritzen, S.-E. 1990: Tertiary caves in Norway; a matter of relief and size. *Cave Science 17*, 31–37.

Lauritzen, S.-E. 1991: Karst resources and their conservation in Norway. *Norsk Geografisk Tidsskrift - Norwegian Journal of Geography 45*, 119–142. https://doi.org/10.1080/00291959108552266.

Lauritzen, S.-E. 2008: Grottolf 4.027, Program for Processing, plotting and analysis of cave survey data.

Lauritzen, S.-E. 2010: *Grotter - Norges ukjente underverden*. Tun Forlag, Oslo, 240 pp.

Lauritzen, S.-E. & Mihevc, A. 2015: Large-passage cross-sections : the A-frame lesson. In: Zupan Hajna, N., Mihevc, A. & Gostincar, P. (eds.). Caves - exploration and studies : program & excursions & UIS & abstracts. 23rd International Karstological School "Classical Karst", Postojna, Slovenia: Karst Research Institute ZRC SAZU.

Lauritzen, S.-E., Baastad, L., Bjørlien, J., Fedje, E. & Holmlund, P. 2005: The Svarthamar cave research project, Fauske, north Norway. *14th International Congress of Speleology, 21–28 August, Athen-Kalamos*, 5 pp.

Leach, D.L., Bradley, D.C., Huston, D., Pisarevsky, S.A., Taylor, R.D. & Gardoll, S.J. 2010: Sediment-hosted lead-zinc deposits in earth history. *Economic Geology 105*, 593–625. https://doi.org/10.2113/gsecongeo.105.3.593.

Lidmar-Bergstrom, K., Naslund, J.O., Ebert, K., Neubeck, T. & Bonow, J.M. 2007: Cenozoic landscape development on the passive margin of northern Scandinavia. *Norwegian Journal of Geology 87*, 181–196.

Mangerud, J. 2004: Ice sheet limits in Norway and on the Norwegian continental shelf. *In* Ehlers, J. & Gibbard, P. (eds.): *Quaternary Glaciations - Extent and Chronology 2*, Elsevier, Amsterdam, pp. 271–294. https://doi.org/10.1016/S1571-0866(04)80078-2.

Martínez-Moreno, F.J., Galindo-Zaldívar, J., Pedrera, A., Teixido, T., Ruano, P., Peña, J.A., González-Castillo, L., Ruiz-Constán, A., López-Chicano, M. & Martín-Rosales, W. 2014: Integrated geophysical methods for studying the karst system of Gruta de las Maravillas (Aracena, Southwest Spain). *Journal of Applied Geophysics 107*, 149–162. https://doi.org/10.1016/j.jappgeo.2014.05.021.

Martínez-Moreno, F.J., Galindo-Zaldívar, J., Pedrera, A., Teixidó, T., Peña, J.A. & González-Castillo, L. 2015: Regional and residual anomaly separation in microgravity maps for cave detection: The case study of Gruta de las Maravillas (SW Spain). *Journal of Applied Geophysics 114*, 1–11. https://doi.org/10.1016/j.jappgeo.2015.01.001.

McMechan, G.A., Loucks, R.G., Mescher, P. & Zeng, X. 2002: Characterization of a coalesced, collapsed paleocave reservoir analog using GPR and well-core data. *Geophysics 67*, 1148–1158. https://doi.org/10.1190/1.1500376.

Milbert, D. 2018: http://geodesyworld.github.io/SOFTS/solid.htm; based on an edited version of the dehanttideinelMJD.f source code by Professor V. Dehant. This code is an implementation of the solid earth tide computation found in section 7.1.2 of the IERS Conventions (2003), IERS Technical Note No. 32. Accessed: 24.05.2018.

Mylroie, J.R. & Mylroie, J.E. 2007: Development of the carbonate island karst model. *Journal Of Cave And Karst Studies 69*, 59–75.

Olesen, O., Brönner, M., Ebbing, J., Gellein, J., Gernigon, L., Koziel, J., Lauritsen, T., Myklebust, R., Pascal, C., Sand, M., Solheim, D. & Usov, S. 2010: New aeromagnetic and gravity compilations from Norway and adjacent areas; methods and applications. *Petroleum Geology Conference Proceedings 7*, 559–586. https://doi.org/10.1144/0070559.

Roberts, D., Heldal, T. & Melezhik, V. 2001: Tectonic structural features of the Fauske conglomerates in the Lovgavlen Quarry, Nordland, Norwegian Caledonides, and regional implications. *Norsk Geologisk Tidsskrift 81*, 245–256.

Roberts, D., Melezhik, V.A. & Heldal, T. 2002: Carbonate formations and early NW-directed thrusting in the highest allochthons of the Norwegian Caledonides: evidence of a Laurentian ancestry. *Journal of the Geological Society, London 159*, 117–120. https://doi.org/10.1144/0016-764901-128.

Skoglund, R.O. & Lauritzen, S.-E. 2010: Morphology and speleogenesis of Okshola, Fauske, Northern Norway; example of a multi-stage network cave in a glacial landscape. *Norwegian Journal of Geology 90*, 123–139.

Styles, P., McGrath, R., Thomas, E. & Cassidy, N.J. 2005: The use of microgravity for cavity characterization in karstic terrains. *Quarterly Journal of Engineering Geology and Hydrogeology 38*, 155–169. https://doi.org/10.1144/1470-9236/04-035.

Valen, V., Lauritzen, S.-E. & Løvlie, R. 1997: Sedimentation in a high-latitude karst cave: Sirijordgrotta, Nordland, Norway. *Norsk Geologisk Tidsskrift 77*, 233–250.

Paper 2 – Increasing reliability of seismic prediction […]

Title: Increasing reliability of seismic prediction of karst morphology, with examples from the Loppa High, Norwegian Continental Shelf.

The paper was submitted to Petroleum Geoscience 21st of November 2019, but returned to main author on the 10th of December 2019 with detailed comments by the editor and termed although "rejected" at that point was invitated for re-submission after revision.

Main objectives of the paper: To provide a better understanding of, and limitations when, interpreting karst from seismic reflection data, exemplified with case studies from Loppa High in the Barents Sea.

Candidate's Contributions: My contribution to this article was the idea for the study, the interpretation of seismic reflection data, compilation of field analogs and writing of the manuscript. My co-supervisors Tore A. Svånå and Christine Fichler and main supervisor Philip Ringrose all contributed to scientific discussion, and improvement of the manuscript.

This article is awaiting publication and is therefore not included.

Karst and potential karst on the Norwegian Continental Shelf – basement and basin cover processes and onshore-offshore perspectives

Prepared for submission to Marine and Petroleum Geology

Authors and affiliations

Name of authors

Terje Solbakk[1*], Christine Fichler[1] and Tore Amund Svånå[2],

Full postal addresses.

[1]Department of Geoscience and Petroleum, Norwegian University of Science and Technology (NTNU), Sem Sælands veg 1, 7491, Trondheim, Norway.

[2]Lilandsveien 290, 8534 Liland, Norway.

*Corresponding author (e-mail: terje.solbakk@ntnu.no)

Abstract

We review karst and paleokarst features for the entire Norwegian Continental Shelf (NCS) showing how karst contributes to the overall porosity and identify the most promising karst plays mainly found in Upper Paleozoic carbonates. Known - and potential karst systems in the sedimentary cover and uppermost crystalline basement are compiled, separately addressing the Barents Sea, the Norwegian Sea, and the North Sea. The compilation is based on reviews and new investigations applying a comprehensive workflow for the mapping of karst potential. Karst morphology (strictly paleokarst) is documented from exploration wells and from seismic interpretations. It has been found that the nature of karst porosity is highly variable. Furthermore, there is significant under-explored karst potential on the NCS, especially in carbonate intervals beneath major unconformities in the Norwegian Sea and the North Sea.

Manuscript: Karst on the Norwegian shelf…. Solbakk *et al.*, 20XXb

The most promising karst plays are found in Upper Paleozoic carbonates found on all three sub-areas of the NCS. Karst development in Late Mesozoic/Early Cenozoic chalk strata may also create generate additional reservoir quality in the eastern North Sea, which is an under-explored part of the NCS. Paleokarst may also be found in certain Caledonian basement terranes on the NCS; as proven by one well in the Norwegian Sea. The paper also identifies other karst plays that have not been proven yet, but which could give rise to enhanced porosity and reservoir improvement. Although meteoric fluids are the primary agents for karstification, hypogene fluids related to deep-seated fault zones could be present and could alter carbonate reservoirs diagenetically. However, hypogene fluids are known to vary in chemical composition, and this fluid chemistry may lead to different types of diagenesis, ranging from host rock dissolution to pore clogging, giving uncertain effects on reservoir quality. Other potential plays include silicate karst and pseudokarst features such as deep weathering, lava tubes and piping.

This article is awaiting publication and is therefore not included.

Synthesis

The scope for this thesis was to integrate conventional seismic interpretation, gravity survey data, field data from analogues and state-of-the-art numerical modeling in order to broaden and increase the understanding of the distribution of porosity and permeability derived from chemical dissolution of rocks (karst). Karst porosity from small scales to the large scales are addressed onshore Norway (Paper 1), the intermediate scale in the offshore setting of the Loppa High, Barents Sea (Paper 2) and the large scale encompassed the entity of both land and offshore areas of Norway (Paper 3). All papers present new workflows combining geophysical methods and geology for karst mapping and prediction. Furthermore, challenges related to distinguishing pseudokarst from karst were addressed in the two offshore papers (Paper 2 and 3, as well as the geophysical imaging problems related to isomorphs (Paper 2).

The combination of geophysical exploration and geological interpretation of karstification onshore and offshore Norway is documented with an offshore case history in Paper 1 and two case histories in Paper 2.

The first case study area includes onshore Norway's largest cave room, within the Svarthammarhola cave system (SHC), located in a Caledonian nappe setting in Nordland. This is the first time microgravimetric data is used for mapping of known and detection of hitherto unknown karst cave passages in Norway.

Gravity field anomalies are caused by negative density contrasts between host rock and karst features. An interpretation approach applicable for challenging geological settings with heterogeneous lithologies has been developed. The workflow covers not only the detection of large cave rooms, but also deals with minor karst features (epikarst) in carbonate rocks. Challenges due to heterogeneous infill of large cavities and variations in carbonate facies are addressed applying 3D forward modeling of surface gravity measurements over the large karst cave complex. The most important result relates to distinct gravity lows, which are interpreted as hitherto unknown and inaccessible cave rooms, some of them of a very large size. These correspond with known cave collapse, and sediment infill features both at the surface and inside the SHC system. This expands the known cave in an eastward and northward direction. Lessons learned from this work are that it is important for future application of the gravity method in complex fold settings to gain a rough understanding of where one can expect possible karstified cavities, at what depth and lateral extent. It is also beneficial to expand the area of interest into the non-karstified area. It is suggested to gather a few longer (regional) gravity profiles in addition to the gravity study grid to capture larger wavelength of the gravity field related to deeper structures, and to gain a better understanding of the background trend of the gravity anomalies. Detailed geological mapping at the surface above the cave and within the cave (where possible) with rock sampling is another necessity. New options for the speleogenesis were discussed based on (1) the SHC's position at the top of the hinge of a large anticline, (2) uncommonly high densities in the area of the hinge and (3) the cave's outstanding size. The hinge of an anticline is commonly is a focus point for fluids migrating from greater depths. However, with present knowledge we cannot distinguish between a meteoric or a hypogene origin for the SHC. The hypogene hypothesis is suggested to be tested in further work by invasive sampling in the known and hidden cave system, combined with further geophysical exploration.

Two offshore areas are investigated in Paper 2, located in the Mid-Carboniferous – Permian carbonates of the Loppa High in the southwestern Barents Sea. Here, the nature of karst features is reviewed, their seismic expression, and potential isomorphs. Recent seismic interpretations of offshore karst on the Norwegian Continental Shelf (NCS) (caves, dolines, and epikarst) by Ahlborn *et al.* (2014), Hunt *et al.* (2003), Hunt *et al.* (2010), Rafaelsen *et al.* (2008), Sayago *et al.* (2012), and Sorento *et al.* (2018) demonstrates that alternative explanations (isomorphs) for the assumed seismic expressions of karst, are rarely addressed.

In these case study areas, we focus on possible traps related to interpreted karst features from seismic data. A new workflow is presented for a systematic, reliable approach for recognition of karst from seismic data, including secondary information. One of the regions gave clear karst expressions on seismic data that were supported by geological arguments, whereas the other region resulted in more equivocal interpretations where alternative models may be valid. Hydrocarbon reservoirs in karstified carbonate rocks are important in a global perspective and have recently been proven on the NCS. The karstification process generally provides excellent porosity and permeability, which ideally will give good acoustic-property contrasts that would make karst features easy to identify from seismic reflection data. Challenges related to the identification of karst elements and karst landforms include the size distribution of the cavities, the resolution capability of seismic data, the geological history leading to different types of karst infill, and the differentiation from other features which give similar seismic expressions (isomorphs). Therefore, identifying karst-like morphology on seismic reflection data alone is not sufficient to prove karstification - the seismic expression needs further support from integrated geological interpretations, and alternative isomorph interpretations need to be assessed. This take-home lesson is perhaps the most important from a hydrocarbon exploration perspective in frontier areas such as the Barents Sea.

Karst at the large scale is addressed by Paper 3, which deals with known karst morphology of onshore Norway and the NCS as well as the karst potential of the NCS. The paper also briefly discusses other elements such as silicate karst and pseudokarst features such as deep weathering, lava tubes, piping, and others. The aim is to get an overview of where to find karst features buried on the NCS, and what kind of karst one might expect to find in these offshore, submerged settings. Karst (paleokarst) features are found in exploration wells on all three sub-areas of the NCS, the karst porosity contribution to the overall porosity of potential reservoir rocks is highly variable. With the experience gained in the case histories, combined with knowledge of karst occurrences onshore and offshore, a broader view has been compiled addressing existing and potential karst areas from the entire Norwegian Continental Shelf (NCS). This is the first publication that reviews and addresses karst on such scale in offshore Norway.

Meteoric fluids stand out as the primary agent for karstification of the submerged rocks of the NCS. Hypogene fluids can theoretically be present under certain conditions, and can, therefore, alter carbonate reservoirs diagenetically, for good or bad, meaning cavity increase or decrease, respectively. Such fluids are often related to deep-seated fault zones. This concept has not yet been proven on the NCS and a new systematic workflow for the detection of such fluid systems is presented for the NCS.

The most promising karst plays are found in Late-Paleozoic limestones in all three sub-areas of the NCS. Karst in chalk may have a potential upside in the eastern North Sea, which is an under-explored part of the NCS. Several limestone levels capped by unconformities are not explored in the Norwegian Sea and the North Sea. Paleokarst may also be found in crustal Caledonian terrane below the sediments; for now, dolomite encountered in one well in the Norwegian Sea (well 6608/8-1, see Paper 3) is the only candidate for a possible Caledonian age. These dolomites have earlier been assigned a Late Permian age (Factpages.npd.no). Targeting reservoirs in Caledonian-age carbonates has not been addressed in the Norwegian Sea. Finally, pseudokarst may give rise to additional offshore plays by enhanced porosity and reservoir improvement.

Seen together, the three papers presented here, have significantly improved methods for the analysis of karst systems both onshore and offshore Norway, using case examples from different areas, and aiming for a more confident interpretation of karstified carbonate bodies. The work offers a framework for future studies of karstified carbonate plays in hydrocarbon exploration. Paper 3 also provides clues to areas where karst is underexplored.

The methods used and workflows developed here are also applicable for investigation of groundwater systems. Finally, there is also a potential application to maturing future karstified carbonate reservoirs for injecting CO_2, methane, and hydrogen, both on- and offshore.

Main conclusions

- Geophysical identification of karst elements and karst landforms is not an easy task, the main challenges relate to the size distribution of the cavities, the resolution capability of the geophysical data, the geological history leading to different types of karst infill, and the differentiation from other features which give similar seismic expressions (isomorphs).
- New workflows for integrated geophysical and geological karst detection are developed for onshore and offshore settings and for different scales illustrated with case studies. This resulted in a better understanding of known karst as well as an assessment of karst potential in both onshore and offshore settings.
- An interpretation approach for microgravimetry is presented, applicable for challenging onshore geological settings with heterogeneous lithologies and karst features located very near below the surface. The workflow covers not only the detection of large cave rooms, but also deals with minor karst features (epikarst) in carbonate rocks.
- Based on microgravimetric interpretation, the Svarthammarhola cave system (SHC) is suggested to be expanded in an eastward and northward direction with hitherto unknown and inaccessible cave rooms, some of them of a very large size. These correspond with known collapse and sediment infill features both at the surface and inside the SHC system.
- An offshore workflow is presented for a systematic, reliable approach for recognition of karst from seismic data, including secondary information and distinction from isomorphs. This workflow is applicable to larger depths and puts higher reliability on the seismic karst interpretation.
- Two areas with karst potential on the Loppa High (southwestern Barents Sea) were identified from interpretations on seismic data: one with clear karst expressions supported by secondary arguments, and one with more equivocal interpretations where alternative models may be valid. The implication of these alternative karst models is shown to be significant for hydrocarbon exploration.
- An overview of karst features is presented for the Norwegian Continental shelf (NCS) together with significant karst features on the Norwegian mainland. For the first time, the entirety of karst (paleokarst) features from wells and seismic reports has been compiled for the Norwegian Continental Shelf (NCS). At least 17 wells (hydrocarbon discoveries counts as one well) and 3 IKU wells hold evidence of karstification. These wells are found all over the NCS on structural highs. The karst porosity contribution to the overall porosity of potential reservoir rocks has shown to be highly variable and

the full spectrum of karst porosity known from onshore analogues is therefore expected.

- Areas with karst potential on the NCS have been derived based on this compilation, combined with mapped karst features from the Norwegian mainland, as well as with common and NCS specific requisites for karstification. The assessment included host rocks of karstification (limestone, dolomite, anhydrite, salt, chert), the conditions and climate during their deposition, their uplift and erosional history, and the fluid system.
- This is also the first time that a systematic workflow for the detection of offshore karstifiable rocks and fluid systems is applied on the entire NCS. The offshore karst occurrences are set in connection to known offshore and onshore karst; possible new karst plays are outlined, related to both meteoric and to hypogene fluids. The results show that there might be an overlooked karst potential on the NCS, of unknown significance.
- The most promising karst plays on the NCS are in Late-Paleozoic carbonates. Karst in chalk may have a potential upside in the eastern North Sea, the latter being an under-explored part of the NCS in so matter. Furthermore, carbonate levels, capped by unconformities, are generally not explored in the Norwegian Sea and the North Sea, but have been more frequently targeted in the southwestern Barents Sea.
- Paleokarst may also be present in the offshore part of the Caledonian basement terrane.

Perspective, future research and potential improvements

Karst porosity is a fascinating and puzzling feature. It is connected to both the land surface (meteoric) as well as detached from it (hypogene). There are still many issues to resolve in detection and visualization of submerged karstified landforms. One needs to keep in mind that meteoric karst landforms do not develop in isolation from other landforms – they are generated in concert with other non-karstic landforms, meaning different processes acting at the same time on the same rock. Therefore, it is always important to consider isomorphs when interpreting karst prone rocks instead of going directly to the assumption of karstification. There is not a fixed relationship with a predetermined ratio of non-karst and karst porosity; this ratio will vary with several factors.

Although the overall 'karst play' on the Norwegian Continental Shelf has been of limited commercial success so far, the comprehensive review complied in Paper 3 should form the basis for future assessments of karstified reservoir formations. Furthermore, even though this Ph.D. work has been performed with funding and perspectives directed towards the Arctic, the developed methods will also apply to many other exploration area targeting karstified reservoirs in submerged settings and complex fold-belts of similar composition as the Norwegian geological settings.

The integration of conventional seismic interpretation, gravity data, field data from analogues and state-of-the-art numerical modeling will result in a new and better understanding of the distribution of rocks with given properties. This insight can have several other applications, mostly for better targeting, thus improving discovery rate in hydrocarbon reservoirs in sedimentary and igneous rocks where superimposed chemical dissolution may lead to better reservoir properties. Karst-prone carbonates are widespread throughout the NCS, and new hydrocarbon plays may well emerge in future.

For field development, these results can improve the well management and well planning, and by that lower the total number of exploration wells and appraisal wells for a given discovery, and subsequently in production. It can help to decide the karst presence more precisely, or no-presence of, of the targeted dissolution properties in rocks. It can also assist on drilling targets – prospects - and may therefore also help to reduce "dusters" – wells with no commercial amounts of hydrocarbon. Furthermore, this is also of value for research on deep weathering, for groundwater exploration and better prediction of groundwater flow in sedimentary basins. Applications may even touch metal ore exploration. Finally, problems related to hazards while drilling for deeper reservoirs through such carbonates may be lowered (Svånå *et al.,* 2018). Therefore, further development of the workflows presented here may have a future option regarding commercialization.

Caves, due to their low energy environment, can also be important sedimentary archives for the natural history of the surrounding area and for the geological history of the cave itself. They are thus vulnerable to destruction by human entry (Lauritzen, 1991; Ford & Williams, 2007). In the Svarthammarhola area, there is an incomplete sedimentary record since glacial erosion has removed and/or redistributed sediments and rocks on the surface (e.g., Andersen, 1975; Mangerud, 2004; Hughes *et al.*, 2015). The implications of this, if further investigations confirm this thesis interpretation of a hidden cave, are important and not without complications. The possibility of encountering sediments and speleothems of a Neogene age or older, susceptible for dating, is intriguing and should be a focus for further work in this area. The hidden continuation of the SHC may contain important and unknown clues, from sediment infill and other speleothems, concerning the natural history of Scandinavia. Due to the vulnerable underground environment and the value of potential natural history data, e.g., zoological, glacial, and vegetational history to be extracted from the cave, a careful and planned investigation must take place to make sure that all possible information is retrieved in a sound, scientific way.

Other play opportunities may emerge from the workflows developed in this thesis. This includes chemical dissolution settings gathered under the term “pseudokarst” (Paper 2). Topics of notable interest include:

1. Deep weathering: This may be regarded as a type of karst, as karst is defined as a chemical dissolution feature, according to Ford & Williams (2007). It is generated by acidic fluids acting on crystalline rocks and associated with tropical climate conditions, and where the rock’s weathering product is an in-situ saprolite with the host-rock fabric still recognizable within the saprolite. If the saprolite is removed, a weathering pattern similar to karst may be imposed on the remaining bedrock (Hall *et al.*, 2015). The Lancaster field west of Shetland produces hydrocarbons from such rocks, and has recently generated renewed interest in this play, as deep weathering seems to be more common than earlier thought. Furthermore, in a setting of where carbonates form a part of the basement, such as in Pre-Cambrian of Northern Norway, both karst and deep weathering may occur and interact.
2. Silicate karst is known from quartzitic consolidated sandstones with primary porosity still intact (Wray & Sauro, 2017). It is, therefore, possible to point to a paleosilicate karst opportunity in Late-Paleozoic (Late Carboniferous) sandstones on the Finnmark Platform/ onshore Finnmark. Here, arenization could have taken place after the consolidation of relatively pure quartz sand deposited in a shallow marine environment with later upheaval.

3. Novel pseudokarst: T. Svånå (pers.comm.) has from seismic data observed possible marine sea cliffs at the northern part of the Loppa High, close to the 7222/1-1 (Aurelia well), which opens for the existence of a novel type of pseudokarst; namely marine abrasion caves.
4. Lava tunnels are likely to be present within the volcanic rocks of the Outer Vøring area, as can be observed from analogue areas onshore (Halliday, 2007). Other pseudokarst occurrences are largely unresolved on the NCS, and their economic importance for hydrocarbon exploration is unknown and would be an interesting item for further research.

Though there is a good progress in the detection of karst utilizing integrated geophysical and geological interpretation as shown in this thesis, there is still a lot of room for further development. This includes especially a more expanded use of joint interpretation of several geophysical methods (see Fig. 1).

For the small-scale onshore example, investigation of the SHC (Paper 1) with a possible prolongation by an already large cave room, could apply to geophysical surveys elsewhere, including shallow seismic methods or other geophysical methods such as electric resistivity tomography (ERT, e.g. Verdet *et al.*, 2020). Such surveys can be conducted prior to perform any invasive methods like drilling or digging into the yet undiscovered or enclosed passage.

Funding

This PhD thesis is funded by the ARCEx project (Research Centre for Arctic Petroleum Exploration, www.arcex.no) which is funded by the Research Council of Norway (grant number 228107) together with 10 academic and 9 industry partners. For Paper 1, the field data campaign was part of the Svarthammar Research Project (Norwegian Research Council, Norpast2; Lauritzen *et al.*, 2005) and initial fieldwork funded through the Department of Earth Sciences, UiB (‘såkornmidler’) to him and Arne Gidskehaug. The task was then merged into a PhD project for Terje Solbakk (TS), supervised by SEL and Walter Wheeler (WW) at the University of Bergen and Center of Integrated Petroleum Research. This task was funded through The Norwegian Research Council for field expenses and salary support (NFR 176132, Paleokarst Reservoirs.

References

Ahlborn, M., Stemmerik, L., Kalsto, T.-K., 2014. 3D seismic analysis of karstified interbedded carbonates and evaporites, Lower Permian Gipsdalen Group, Loppa High, southwestern Barents Sea. Marine and Petroleum Geology 56, 16-33, DOI: 10.1016/j.marpetgeo.2014.02.015.

Al-Marzouqi, M.I., Budebes, S., Sultan, E., Bush, I., Griffiths, R., Gzara, K.B.M., Ramamoorthy, R., Husser, A., Jeha, Z., Roth, J., Montaron, B., Narhari, S.R., Singh, S.K., Poirier-Coutansais, X., 2010. Resolving carbonate complexity. Oilfield Review 22, 40-55.

Andersen, B.G., 1975. Glacial geology of northern Nordland, North Norway. Universitetsforlaget, Trondheim - Oslo, Norway.

Ardestani, V.E., 2008. Modelling the karst zones in a dam site through micro-gravity data*. Exploration Geophysics 39, 204-209, DOI: https://doi.org/10.1071/EG08022.

Barrows, L., Fett, J.D., 1985. A high-precision gravity survey in the Delaware Basin of southeastern New Mexico. Geophysics 50, 825-833, DOI: 10.1190/1.1441957.

Bauer, M., Tóth, T.M., 2017. Characterization and DFN modelling of the fracture network in a Mesozoic karst reservoir, Gomba oilfield, paleogene basin, Central Hungary. Journal of Petroleum Geology 40, 319-334, DOI: 10.1111/jpg.12678.

Beres, M., Luetscher, M., Olivier, R., 2001. Integration of ground-penetrating radar and microgravimetric methods to map shallow caves. Journal of Applied Geophysics 46, 249-262, DOI: http://dx.doi.org/10.1016/S0926-9851(01)00042-8.

Bonacci, O., Andrić, I., Yamashiki, Y., 2014. Hydrology of Blue Lake in the Dinaric karst. Hydrological Processes 28, 1890-1898, DOI: 10.1002/hyp.9736.

Bourdon, L., Coca, S., Alessio, L., 2004. Karst Identification and Impact on Development Plan, SPE Asia Pacific Oil and Gas Conference and Exhibition. Society of Petroleum Engineers, Perth, Australia, DOI: 10.2118/88520-MS.

Braitenberg, C., Sampietro, D., Pivetta, T., Zuliani, D., Barbagallo, A., Fabris, P., Rossi, L., Fabbri, J., Mansi, A.H., 2016. Gravity for Detecting Caves: Airborne and Terrestrial Simulations Based on a Comprehensive Karstic Cave Benchmark. Pure and Applied Geophysics 173, 1243-1264, DOI: 10.1007/s00024-015-1182-y.

Butler, D.K., 1984. Microgravimetric and gravity gradient techniques for detection of subsurface cavities. GEOPHYSICS 49, 1084-1096, DOI: 10.1190/1.1441723.

Bøe, R., Fossen, H., Smelror, M., 2010. Mesozoic sediments and structures onshore Norway and in the coastal zone. Bulletin - Norges Geologiske Undersøkelse 450, 15-32.

Chico, R.J., 1964. Detection of caves by gravimetry. International Journal of Speleology 1, 101-108.

Clark, D.N., 1986. The distribution of porosity in Zechstein carbonates. Geological Society Special Publications 23, 121-149, DOI: https://doi.org/10.1144/GSL.SP.1986.023.01.09.

Corbel, J., 1957. Les karsts du nord-ouest de l'Europe et de quelques regions de comparai son: etude sur le role du climat dans l'erosion des calcaires. IER, Lyon.

Craig, D.H., 1990. Yates and other Guadalupian (Kazanian) oil fields, U. S. Permian Basin. Geological Society Special Publications 50, 249-263, https://doi.org/10.1144/GSL.SP.1990.050.01.12.

Dentith, M., Mudge, S.T., 2014. Geophysics for the Mineral Exploration Geoscientist. Cambridge University Press.Ford, D., Williams, P.D., 2007. Karst hydrogeology and geomorphology. John Wiley & Sons.

Eliassen, A., Talbot, M.R., 2005. Solution-collapse breccias of the Minkinfjellet and Wordiekammen Formations, Central Spitsbergen, Svalbard; a large gypsum palaeokarst system. Sedimentology 52, 775-794, DOI: https://doi.org/10.1111/j.1365-3091.2005.00731.x.

Faleide, J.I., Bjørlykke, K., Gabrielsen, R.H., 2015. Chapter 25 - Geology of the Norwegian continental shelf, in: Bjørlykke, K. (Ed.), Petroleum Geoscience. Springer, pp. 603-637.

Faleide, J.I., Tsikalas, F., Breivik, A.J., Mjelde, R., Ritzmann, O., Engen, Ø., Wilson, J., Eldholm, O., 2008. Structure and evolution of the continental margin off Norway and the Barents Sea. Episodes 31, 82-91.

Ford, D., Williams, P.D., 2007. Karst hydrogeology and geomorphology. John Wiley & Sons.

Ford, D.C., 1995. Paleokarst as a target for modern karstification. Carbonate Evaporite 10, 138-147, DOI: 10.1007/BF03175399.

Fournillon, A., Bellentani, G., Moccia, A., Jumeaucourt, C., Terdich, P., Siliprandi, F., Peruzzo, F., 2017. Characterization of a Paleokarstic Oil Field (Rospo Mare, Italy): Sedimentologic and Diagenetic Outcomes, and Their Integration in Reservoir Simulation, in: Renard, P., Bertrand, C. (Eds.), EuroKarst 2016, Neuchâtel: Advances in the Hydrogeology of Karst and Carbonate Reservoirs. Springer International Publishing, Cham, pp. 47-55, DOI: 10.1007/978-3-319-45465-8_5.

Hall, A.M., Sarala, P., Ebert, K., 2015. Late Cenozoic deep weathering patterns on the Fennoscandian shield in northern Finland: a window on ice sheet bed conditions at the onset of Northern Hemisphere glaciation. Geomorphology 246, 472-488, 10.1016/j.geomorph.2015.06.037.

Halliday, W.R., 2007. Pseudokarst in the 21st century. Journal of Cave and Karst Studies 69, 103-113.

Haugane, E., Grønlie, A., 1988. Tertiary caves in Nordland, Norway. Cave Science 15, 93-97.

Horn, G., 1947. Karsthuler i Nordland. Norges geologiske undersøkelse 165, 77.

Hughes, A.L.C., Gyllencreutz, R., Lohne, Ø.S., Mangerud, J., Svendsen, J.I., 2015. The last Eurasian ice sheets – a chronological database and time-slice reconstruction, DATED-1. Boreas, DOI: 10.1111/bor.12142.

Hunt, D., Colpaert, A., Miquelis, F., Graham-Wall, B., Pajchel, J., Lukasik, J., Rafaelsen, B., Avu, A., Patton, G., 2010. Seismic geomorphology of paleokarst systems in Paleozoic carbonates, Norwegian Barents Sea, in: Wood, L.J., Simo, T.T., Rosen, N.C. (Eds.), 30th Annual GCSSEPM Foundation BoB F Perkins Research Conference 2010. Society of Economic Paleontologists, Gulf Coast Section (GCSSEPM) Foundation, Houston, Texas, USA, pp. 184-206.

Hunt, D., Elvebakk, G., Rafaelsen, B., Pajchel, J., Hogstad, K., Robak, H., Randen, T., 2003. Palaeokarst Recognition & 3D Distribution: New Insights From The Upper Palaeozoic, Loppa High, Barents Sea, EAGE 65th conference & Exhibition, Stavanger, Norway, p. 4.

Jacob, T., Chery, J., Bayer, R., Le Moigne, N., Boy, J.-P., Vernant, P., Boudin, F., 2009. Time-lapse surface to depth gravity measurements on a karst system reveal the dominant role of the epikarst as a water storage entity. Geophysical Journal International 177, DOI: 347-360, 10.1111/j.1365-246X.2009.04118.x.

Kaufmann, G., Nielbock, R., Romanov, D., 2015. The Unicorn Cave, Southern Harz Mountains, Germany: From known passages to unknown extensions with the help of geophysical surveys. Journal of Applied Geophysics 123, 123-140, DOI: http://dx.doi.org/10.1016/j.jappgeo.2015.10.004.

Kaufmann, G., Romanov, D., 2009. Geophysical investigation of a sinkhole in the northern Harz foreland (North Germany). Environmental Geology 58, 401-405, DOI: 10.1007/s00254-008-1598-0.

Kerans, C., 1988. Karst-controlled reservoir heterogeneity in Ellenburger Group carbonates of West Texas. AAPG Bulletin 72, 1160-1183, DOI: 10.1306/703C996F-1707-11D7-8645000102C1865D.

Klimchouk, A., 2015. The karst paradigm: changes, trends and perspectives. Acta Carsologica 44, 289-313.

Klimchouk, A., 2018. Advances in understanding hypogene karst, in: K.W., S., G., V. (Eds.), Hypogene Karst of Texas. Texas Speleological Survey, pp. 3-20.

Korneliussen, A., Raaness, A., Gautneb, H., 2013. Chemical and mineralogical characterisation of carbonate deposits in Norway, NGU report. Geological survey of Norway, Trondheim, Norway, p. 169.

Kovacova, T., 2010. Geophysical investigation of faults and fractures in Upper-Palaeozoic carbonate build-ups at the Loppa High, SW Barents Sea, Department of Geology. University of Tromsø, Tromsø.

Landrø, M., Amundsen, L., 2018. Introduction to exploration geophysics with Recent Advances. Bivrost, p. 341.

Lapointe, P.A., Soudet, H.J., Courme, B., 2002. Karst-controlled reservoirs, identification and prediction of reservoir characteristics distribution through seismic, well data and outcrops, in: Gabrovsek, F. (Ed.), Evolution of karst; from prekarst to cessation; proceedings. Zalozba ZRC, pp. 435-443.

Larsen, B.T., Olaussen, S., Sundvoll, B., Heeremans, M., 2006. Vulkaner, forkastninger og ørkenklima - Osloriften og Nordsjøen i karbon og perm, 359-251 millioner år, in: Ramberg, I.B., Bryhni, I., Nøttvedt, A. (Eds.), Landet blir til - Norges Geologi. Norsk Geologisk Forening, pp. 284-327.

Larssen, G., Elvebakk, G., Henriksen, L., Kristensen, S., Nilsson, I., Samuelsberg, T., Svånå, T., Stemmerik, L., Worsley, D., 2002. Upper Palaeozoic lithostratigraphy of the Southern Norwegian Barents Sea, Norwegian Petroleum Directorate Bulletin, Stavanger, Norway, p. 145.

Lauritzen, S.-E., 1986. Kvithola At Fauske, Northern Norway - An Example Of Ice-Contact Speleogenesis. Norsk Geologisk Tidsskrift 66, s. 153-161.

Lauritzen, S.-E., 1990. Tertiary caves in Norway; a matter of relief and size. Cave Science 17, s. 31-37.

Lauritzen, S.-E., 1991. Karst resources and their conservation in Norway. Norsk Geografisk Tidsskrift - Norwegian Journal of Geography 45, 119-142, DOI: 10.1080/00291959108552266.

Lauritzen, S.-E., 2001. Marble Stripe Karst of the Scandinavian Caledonides: an end-member in the contact karst spectrum. Acta Carsologica 30/2, s. 47-79.

Lauritzen, S.E., 2006. Grotolf, 4.023 ed, Bergen, For visualization of cave surveying data.

Lauritzen, S.-E., 2008. Speleogenesis and karst landform development in central Scandinavia; an overview, 33rd International Geological Congress, Oslo, Norway.

Lauritzen, S.-E., 2010. Grotter - Norges ukjente underverden. Tun Forlag, Oslo.

Lauritzen, S.-E., Baastad, L., Bjørlien, J., Fedje, E., Holmlund, P., 2005. The Svarthamar cave research project, Fauske, north Norway, 14th International Congress of Speleology. UiS, Athen-Kalamos p. 5.

Lauritzen, S.-E., Dahlgren, S.O., 2017. Pre-Quaternary, hypogenetic caves in south Norway, 17th International Congress of Speleology 2ed. Australian Speleological Federation Inc, Sydney, Australia.

Lomando, A.J., Harris, P.M., Orlopp, D.E., 1993. Casablanca Field, Tarragona Basin, offshore Spain; a karsted carbonate reservoir. SEPM Core Workshop 18, 201-225.

Loucks, R.G., 1999. Paleocave carbonate reservoirs; origins, burial-depth modifications, spatial complexity, and reservoir implications. AAPG Bulletin 83, 1795-1834.

Lucia, F.J., 2007. Carbonate reservoir characterization; an integrated approach. Springer, Berlin, Federal Republic of Germany.

Mangerud, J., 2004. Ice sheet limits in Norway and on the Norwegian continental shelf, in: Ehlers, J., Gibbard, P. (Eds.), Quaternary Glaciations - Extent and Chronology. Elsevier, Amsterdam., pp. 271-294.Ardestani, V.E., 2008. Modelling the karst zones in a dam site through micro-gravity data*. Exploration Geophysics 39, 204-209.

Martínez-Moreno, F.J., Galindo-Zaldívar, J., Pedrera, A., Teixidó, T., Peña, J.A., González-Castillo, L., 2015. Regional and residual anomaly separation in microgravity maps for cave detection: The case study of Gruta de las Maravillas (SW Spain). Journal of Applied Geophysics 114, 1-11, DOI: 10.1016/j.jappgeo.2015.01.001.

Martínez-Moreno, F.J., Galindo-Zaldívar, J., Pedrera, A., Teixido, T., Ruano, P., Peña, J.A., González-Castillo, L., Ruiz-Constán, A., López-Chicano, M., Martín-Rosales, W., 2014. Integrated geophysical methods for studying the karst system of Gruta de las Maravillas (Aracena, Southwest Spain). Journal of Applied Geophysics 107, 149-162, DOI: http://dx.doi.org/10.1016/j.jappgeo.2014.05.021.

Martinsen, O.J., Nøttvedt, A., 2006. Av havet stiger landet - Paleogen og neogen (kenozoikum), kontinentene av i dag formes; 66-2,7 millioner år, in: Ramberg, I.B., Bryhni, I., Nøttvedt, A. (Eds.), Landet blir til - Norges Geologi. Norsk Geologisk Forening, pp. 440-477.

Migon, P., Lidmar-Bergström, K., 2002. Deep weathering through time in central and northwestern Europe: problems of dating and interpretation of geological record. Catena 49, 25-40, DOI: 10.1016/S0341-8162(02)00015-2.

Nakrem, H.A., Worsley, D., 2006. Jordens eldste oldtid - kambrium, ordovicium og silur - et yrende liv i havet; 542-416 millioner år, in: Ramberg, I.B., Bryhni, I., Nøttvedt, A. (Eds.), Landet blir til - Norges Geologi. Norsk Geologisk Forening, pp. 148-177.

Nordgulen, Ø., Andresen, A., 2006. Jordas urtid - De eldste bergarter dannes; 4600-850 millioner år, in: Ramberg, I.B., Bryhni, I., Nøttvedt, A. (Eds.), Landet blir til - Norges Geologi. Norsk Geologisk Forening, pp. 62-119.

Osborne, R.A.L., 2000. Paleokarst and its significance for speleogenesis, in: Klimchouk, A.B., Ford, D.C., Palmer, A.N., Dreybrodt, W. (Eds.), Speleogenesis evolution of karst aquifers. National Speleological Society, Huntsville, AL, United States, 113-123.

Palmer, A.N., 2011. Distinction between epigenic and hypogenic maze caves. Geomorphology 134, 9-22, DOI: 10.1016/j.geomorph.2011.03.014.

Rafaelsen, B., Elvebakk, G., Andreassen, K., Stemmerik, L., Colpaert, A., Samuelsberg, T.J., 2008. From detached to attached carbonate buildup complexes - 3D seismic data from the upper Palaeozoic, Finnmark Platform, southwestern Barents Sea. Sedimentary Geology 206, 17-32, DOI: https://doi.org/10.1016/j.sedgeo.2008.03.001.

Sayago, J., 2014. Late Paleozoic basin analysis of the Loppa High and Finnmark Platform in the Norwegian Barents Sea: integration of seismic attributes and seismic sequence stratigraphy, Mathematisch-Naturwissenschaftlichen Fakultät. Universität Potsdam, Potsdam, p. 119.

Sayago, J., Di Lucia, M., Mutti, M., Cotti, A., Sitta, A., Broberg, K., Przybylo, A., Buonaguro, R., Zimina, O., 2012. Characterization of a deeply buried paleokarst terrain in the Loppa High using core data and multiattribute seismic fades classification. AAPG Bulletin 96, 1843-1866, DOI: 10.1306/02271211137.

Sayago, J., Di Lucia, M., Mutti, M., Sitta, A., Cotti, A., Frijia, G., 2018. Late Paleozoic seismic sequence stratigraphy and paleogeography of the paleo-Loppa High in the Norwegian Barents Sea. Marine and Petroleum Geology 97, 192-208, DOI: 10.1016/j.marpetgeo.2018.05.038.

Schindelin, J., Arganda-Carreras, I., Frise, E., Kaynig, V., Longair, M., Pietzsch, T., Preibisch, S., Rueden, C., Saalfeld, S., Schmid, B., Tinevez, J.-Y., White, D.J., Hartenstein, V., Eliceiri, K., Tomancak, P., Cardona, A., 2012. Fiji: an open-source platform for biological-image analysis. Nature Methods 9, 676-682, DOI: 10.1038/nmeth.2019.

Shi, H.X., Peng, G.X., Zheng, D.M., Zhang, L.J., Li, H., Li, G.H., Yang, P.F., Duan, W.S., Chen, M., Zhang, H., Yang, S., Wang, P., Xue, F.J., Liu, X., 2014. Integration of surface seismic and well information to improve drilling success for onshore carbonate caves. European Association of Geoscientists and Engineers (EAGE), DOI: 10.3997/2214-4609.20141362.

Skoglund, R.Ø., Lauritzen, S.E., Gabrovsek, F., 2010. The impact of glacier ice contact and subglacial hydrochemistry on evolution of maze caves; a modelling approach. Journal of Hydrology 388, 157-172, DOI: 10.1016/j.jhydrol.2010.04.037.

Smelror, M., Petrov, O., Larssen, G.B., Werner, S., 2009. Atlas - Geological history of the Barents Sea. Norges Geologiske Undersøkelse, pp. 1-135.

Smith, M.P., Soper, N.J., Higgins, A.K., Rasmussen, J.A., Craig, L.E., 1999. Palaeokarst systems in the Neoproterozoic of eastern North Greenland in relation to extensional tectonics on the Laurentian Margin. Journal of the Geological Society of London 156, Part 1, 113-124, DOI: 10.1144/gsjgs.156.1.0113.

Solbakk, T., Fichler, C., Svånå, T.A., 20XXb. Known karst and karst potential on the Norwegian Continental Shelf – processes in sediments and basement with onshore-offshore perspectives. [To be submitted] NTNU, Trondheim.

Solbakk, T., Fichler, C., Wheeler, W.H., Lauritzen, S.-E., Ringrose, P., 2018. Detecting multiscale karst features including hidden caves using microgravimetry in a Caledonian nappe setting: Mefjell massif, Norway. Norwegian Journal of Geology 98, 359-378, DOI: https://dx.doi.org/10.17850/njg98-3-04.

Solbakk, T., Svånå, T., Fichler, C., Ringrose, P.S., 20XXa. Increasing reliability of seismic prediction of karst morphology, with examples from the Loppa High, Norwegian Continental Shelf. [submitted to Petroleum Geoscience], NTNU, Trondheim.

Sorento, T., Stemmerik, L., Olaussen, S., 2018. Upper Permian carbonates at the northern edge of the Zechstein basin, Utsira High, Norwegian North Sea. Marine and Petroleum Geology 89, 635-652, DOI: https://doi.org/10.1016/j.marpetgeo.2017.10.030.

Stemmerik, L., Elvebakk, G., Worsley, D., 1999. Upper Palaeozoic carbonate reservoirs on the Norwegian arctic shelf; delineation of reservoir models with application to the Loppa High. Petroleum Geoscience 5, 173-187.

Stemmerik, L., Worsley, D., 2005. 30 years on; Arctic upper Palaeozoic stratigraphy, depositional evolution and hydrocarbon prospectivity. Norwegian Journal of Geology 85, 151-168.

Styles, P., McGrath, R., Thomas, E., Cassidy, N.J., 2005. The use of microgravity for cavity characterization in karstic terrains. Quarterly Journal of Engineering Geology and Hydrogeology 38, 155-169, DOI: 10.1144/1470-9236/04-035.

Svånå, T., Gjørv, B., Larssen, B., 2018. Boring i karbonatformasjoner med karst og åpne sprekker, Rapport. Acona, DOI: http://dx.doi.org/10.1016/j.marpetgeo.2015.10.015.

Tian, F., Jin, Q., Lu, X., Lei, Y., Zhang, L., Zheng, S., Zhang, H., Rong, Y., Liu, N., 2016. Multi-layered ordovician paleokarst reservoir detection and spatial delineation: A case study in the Tahe Oilfield, Tarim Basin, Western China. Marine and Petroleum Geology 69, 53-73.

Vahrenkamp, V.C., David, F., Duijndam, P., Newall, M., Crevello, P., 2004. Growth architecture, faulting, and karstification of a middle Miocene carbonate platform, Luconia Province, offshore Sarawak, Malaysia. AAPG Memoir 81, 329-350, DOI: https://doi.org/10.1306/M81928.

Verdet, C., Sirieix, C., Marache, A., Riss, J., Portais, J.-C., 2020. Detection of undercover karst features by geophysics (ERT) Lascaux cave hill. Geomorphology 360. DOI: https://doi.org/10.1016/j.geomorph.2020.107177.

Wray, R.A.L., Sauro, F., 2017. An updated global review of solutional weathering processes and forms in quartz sandstones and quartzites. Earth-Sci Rev 171, 520-557, DOI: https://doi.org/10.1016/j.earscirev.2017.06.008.

Xu, C., Di, B., Wei, J., 2016. A physical modeling study of seismic features of karst cave reservoirs in the Tarim Basin, China. Geophysics 81, 31-41, DOI: https://doi.org/10.1190/geo2014-0548.1.

Yu, J., Li, Z., Yang, L., Han, Y., 2018. Model identification and control of development of deeply buried paleokarst reservoir in the central Tarim Basin, northwest China. Journal of Geophysics and Engineering 15, 576-592, DOI: https://doi.org/10.1088/1742-2140/aa9c00.

Zeng, H., Loucks, R., Janson, X., Wang, G., Xia, Y., Yuan, B., Xu, L., 2011. Three-dimensional seismic geomorphology and analysis of the Ordovician paleokarst drainage system in the central Tabei Uplift, northern Tarim Basin, western China. AAPG Bulletin 95, 2061-2083, 10.1306/03111110136.

Appendix: Other publications and presentations

A1: Scientific note published in Norwegian Journal of Geology

This cooperation emerged after an evening trip to Stjørdal museum Værnes, where two roof slates found in the museum's archives were closer examined. I participated in the initial examination, made a figure, and edited the manuscript.

Title: Notes on Ordovician graptolites, nautiloids and trace fossils from Lånke, Central Norwegian Caledonides

Authors: Morten Smelror[1], Terje **Solbakk**[2], Bjørn Ivar Rindstad[1], Helle Vangen Stuedal[3] & Karstein Hårsaker[4]

[1]Geological Survey of Norway, P.O. Box 6315 Torgarden, 7491 Trondheim, Norway
[2]Norwegian University of Science and Technology, S.P. Andersens vei 15B, 7491 Trondheim, Norway
Present address: Geological Survey of Norway, P.O.Box 6315 Torgarden, 7491 Trondheim, Norway
[3]Stjørdal Museum Værnes, Prestmovegen 2, 7500 Stjørdal, Norway
[4]NTNU Vitenskapsmuseet, Erling Skakkes gate 47A, 7012 Trondheim, Norway

Abstract

Graptolites and trace fossils typical of deep-water environments are found on phyllitic roofing slates kept in the collections of the Stjørdal Museum Værnes, Trøndelag. The slates probably come from abandoned local quarries in the Stjørdal and Lånke districts. The fossils from Lånke also include some grap-tolites and poorly preserved nautiloids stored at the NTNU Vitenskapsmuseet, Trondheim. The graptolites indicate a Katian age, while the trace fossil assemblages compare to similar assemblages reported from the Middle–Late Ordovician Vuddudalen and Lower Hovin groups and the mostly Silurian Ekne Group of the Central Norwegian Caledonides.

Doi: https://dx.doi.org/10.17850/njg100-2-2.

A2: Abstract Winter conference in geology 2020

As part of a field excursion to Tromsdalen limestone quarry, Verdal in Trøndelag, samples were taken of karst infill sediments discovered under the visit. Microscopy analyses this autumn revealed Mesozoic microfossils and palynomorps in the infill sediments. This work is still on-going. Preliminary results were presented at the Winter conference in geology in January 2020 by the Terje Solbakk.

Title: Mesozoic microfossils recovered from karstified limestone in the Tromsdalen Quarry, Trøndelag – Traces of an unknown inlier basin along the Møre Trøndelag Fault Zone?

Terje **Solbakk[1]***, Harald Brunstad[2], Ingard Throndsen[3] & Morten Smelror[4]

[1] Institutt for geovitenskap og petroleum, NTNU
[2]Lundin Petroleum Norway AS
[3]Applied Petroleum Technology AS
[4]Norges geologiske undersøkelse
*email: Terje.Solbakk@ntnu.no

Analyses of unconsolidated sediments infilled in karstified, Ordovician limestone of the Vuddudalen Group, Central Norwegian Caledonides, in the Tromsdalen Quarry near Verdal, Trøndelag, revealed reworked Mesozoic palynomorphs, together with younger Quaternary/recent pollen and spores. Karst features are probably of Late Quaternary age, developed in a relatively pure limestone of more than 90 % calcite. The infill sediments comprise a greyish diamicton overlying red-brownish clay and silt. Along the Møre-Trøndelag Fault Complex (MTFC), Mesozoic submerged basins are proven in Edøyfjorden by drilling and in Beitstadfjorden with seismic reflection data. Mesozoic and Upper Paleozoic sediments are also found preserved in a fault zone running parallel to the MTFC beneath Frøyfjorden. Erratics with Jurassic plant fossils and coals are found at Verran at the west coast of Beitstadfjorden. Also, reworked Jurassic and Early Cretaceous dinoflagellate cysts are recovered from Quaternary cores off Tautra and Verdal. The reworked microfloras from the karst infill sediments at the Tromsdalen Quarry comprises Jurassic-Cretaceous taxa; likely also including species of Late Cretaceous age. To our knowledge Late Cretaceous fossils have never before been recorded from mainland Norway. These discoveries point to the presence of an unknown, Mesozoic inlier basin to the E of the inner part of the Trondheimsfjorden basin. Our primary model explaining the presence of these infill sediments is that they belong to a Late Quaternary/Holocene glacio-fluvial infill episode, and is derived from a larger, upstream provenance somewhere to the east of Tromsdalen. However, there is a need for follow up investigations.

A3: Presentations held at conferences and workshops

(presenters in bold) Preliminary results were communicated as presentations at relevant conferences and are listed below.

1. **Aizprua Luna**, C.A., Solbakk, T., Johansen, S.E., 2016. Insights on pore systems in Permian Carbonates in the Barents Sea using effective medium theory models, Exploring and Exploiting Carbonate Reservoirs, Bari, Italy.
2. **Solbakk**, T., 2015. Submerged weathering heights of the Arctic, PhD seminar Spring 2015, Scandic hotel Lerkendal, Trondheim.
3. **Solbakk**, T., 2016. Dypvitring på norsk sokkel, Leiromvandling av berggrunnen - hvor og hvorfor?, NGU, Trondheim, Norway.
4. **Solbakk**, T., Fichler, C., Lauritzen, S.-E., Wheeler, W.H., Ringrose, P., 2017. Identifying hidden cave systems using gravimetric mapping: A case study from cave Svarthammarhola, Nordland, Norway, iMagine - Arctic Days 2017, Svolvær.
5. **Solbakk**, T., Fichler, C., Svånå, T.A., Ringrose, P., 2019. Different aspects of detection of karstified reservoirs - case examples from seismic interpretation, ARCEx Annual Conference 2019, Sommarøy, Troms.
6. **Solbakk**, T., Fichler, C., Wheeler, W., Lauritzen, S.-E., Ringrose, P.S., 2017. Challenges in Identifying Karst Porosity in a Caledonian Nappe Setting Using Gravimetric Mapping, 23rd European Meeting of Environmental and Engineering Geophysics. EAGE, Malmö, Sweden, p. 4.
7. **Solbakk**, T., Johansen, S.E., Svånå, T., Aizprua Luna, C.A., 2016. Karstified reservoir rocks in the Arctic – Loppa High, ARCEx Conference 2016, Clarion Hotel The Edge, Tromsø.
8. **Solbakk**, T., Luna, C.A.A., Johansen, S.E., Svånå, T.A., 2016. Characterization of karst – a new approach?, Exploring & Exploiting Carbonate Reservoirs, Bari.
9. **Solbakk**, T., Luna, C.A.A., Johansen, S.E., Svånå, T.A., 2016. Pitfalls when interpreting karst from seismic images. Examples from the Norwegian shelf, 24th International Karstological School "Classical Karst" - Paleokarst, Postojna, Slovenia.
10. **Solbakk, T**., Brunstad, H., Throndsen, I., Smelror., M. Mesozoic microfossils recovered from karstified limestone in the Tromsdalen Quarry, Trøndelag – Traces of an unknown inlier basin along the Møre Trøndelag Fault Zone? Nordic Geologic Wintermeeting 2020, Oslo, Norway.

A4: Other presentations held

1. **Solbakk**, T, Øverland, J. A., 2017. Kvæfjordkull og andre merkelige fremmedsteiner, Trøndelag amatørgeologiske forening (TAGF), member meeting, 5th April 2017, Tyholt, Trondheim.
2. **Solbakk**, T., 2017. Norske grotter - fra land til kontinentalsokkel, Norsk grottedykkerforbund (NGDF), annual meeting, 22nd April 2017 Lade, Trondheim.

A5: Public outreach (already published)

The candidate published geology themed blog posts regularly at geoforskning.no as part of the mandatory PhD work for the institute, in addition to one blog post at ngu.no and three articles and a book review, all listed below. The candidate is also active with geological themed posts and more on Twitter (@terjesolbakk) and Instagram (@terjesolbakk77).

1. Larsen Angvik, T., **Solbakk**, T. & Bunkholt, I. 2016: Isbjørnfare i papirgrotte. Link: http://www.ngu.no/blogg/isbjornfare-i-papirgrotte
2. **Solbakk**, T. 2015: Belemnittmysteriet under Svartisen. In: Geo. GeoPublishing, co/NGU, 7491 Trondheim, 18-21. http://geoforskning.no/nyheter/grunnforskning/1097-belemnittmysteriet-under-svartisen.
3. **Solbakk**, T., 2015. Bumerket oppunder Kvalvasstinden, Årbok for Beiarn 2015.
4. **Solbakk**, T. 2015: Oppdatert lærebok i Petroleumsgeovitenskap. In: Geo. GeoPublishing, co/NGU, 7491 Trondheim, 30-31.
5. **Solbakk**, T. 2015: Svevende flyttblokker. http://geoforskning.no/blogg/item/svevende-flyttblokker.
6. **Solbakk**, T. 2015: Norske huleboere. http://www.geoforskning.no/blogg/item/norske-huleboere.
7. **Solbakk**, T. 2015: Et mulig oljesig ved Finnmarkskysten. http://geoforskning.no/blogg/item/et-mulig-oljesig-ved-finnmarkskysten.
8. **Solbakk**, T. 2015: Arktisk petroleumsutforskning. http://geoforskning.no/blogg/item/arktisk-petroleumsutforskning.
9. **Solbakk**, T. 2016: Annerledesleira ved Sandstrand. http://geoforskning.no/blogg/item/annerledesleira-ved-sandstrand.
10. **Solbakk**, T. 2016: Nord-Europa – hvor er nå det? http://www.geoforskning.no/blogg/item/myter-geologi-og-nyheter
11. **Solbakk**, T., 2016. Om ei nybygd steinbu og en ukjent steinmur i fjellet opp mot Gråtåtinden og Kvalvasstinden, Årbok for Beiarn 2016

12. **Solbakk**, T. 2016: Saltvannskaffe langs Nordlandskysten. http://geoforskning.no/blogg/item/saltvannskaffe-langs-nordlandskysten.
13. **Solbakk**, T. 2016: Myter, geologi og nyheter. http://www.geoforskning.no/blogg/item/myter-geologi-og-nyheter
14. **Solbakk**, T. 2016: Et undersjøisk oppkomme på strandflaten. http://www.geoforskning.no/blogg/item/et-undersjoisk-oppkomme-pa-strandflaten
15. **Solbakk**, T. & Hocking, W.P. 2016: Anoksiske vann – en reise i dypet og en reise i geologisk tid. http://www.geoforskning.no/blogg/item/saltvannskaffe-langs-nordlandskysten
16. Thomsen, E. & **Solbakk**, T. 2017: Nord-norske oljeeventyr. In: Ottar no. 315, Tromsø, p. 3-10.